In compliance with the
Canadian Privacy Legislation
some supporting forms
may have been removed from
this dissertation.

While these forms may be included
in the document page count,
their removal does not represent
any loss of content from the dissertation.

UNIVERSITY OF ALBERTA

USE OF STRUCTURED PACKING AS A DUALFLOW TRAY IN DISTILLATION

by

JASON PATRICK KACHUR

A thesis submitted to the Faculty of Graduate Studies and Research in partial fulfillment of the requirements for the degree of **Master of Science.**

in

CHEMICAL ENGINEERING

Department of Chemical and Materials Engineering

Edmonton, Alberta

Fall, 2003

National Library
of Canada

Acquisitions and
Bibliographic Services

395 Wellington Street
Ottawa ON K1A 0N4
Canada

Bibliothèque nationale
du Canada

Acquisisitons et
services bibliographiques

395, rue Wellington
Ottawa ON K1A 0N4
Canada

Your file Votre référence
ISBN: 0-612-87793-0
Our file Notre référence
ISBN: 0-612-87793-0

The author has granted a non-exclusive licence allowing the National Library of Canada to reproduce, loan, distribute or sell copies of this thesis in microform, paper or electronic formats.

The author retains ownership of the copyright in this thesis. Neither the thesis nor substantial extracts from it may be printed or otherwise reproduced without the author's permission.

L'auteur a accordé une licence non exclusive permettant à la Bibliothèque nationale du Canada de reproduire, prêter, distribuer ou vendre des copies de cette thèse sous la forme de microfiche/film, de reproduction sur papier ou sur format électronique.

L'auteur conserve la propriété du droit d'auteur qui protège cette thèse. Ni la thèse ni des extraits substantiels de celle-ci ne doivent être imprimés ou aturement reproduits sans son autorisation.

Canada

UNIVERSITY OF ALBERTA

LIBRARY RELEASE FORM

NAME OF AUTHOR: **Jason Patrick Kachur**

TITLE OF THESIS: **Use of Structured Packing as a Dualflow Tray in Distillation**

DEGREE: **Master of Science**

YEAR THIS DEGREE GRANTED: **2003**

Permission is hereby granted to the University of Alberta Library to reproduce single copies of this thesis and to lend or sell such copies for private, scholarly or scientific research purposes only.

The author reserves all other publication and other rights in association with the copyright in the thesis, and except as herein before provided, neither the thesis nor any substantial portion thereof may be printed or otherwise reproduced in any material form whatever without the author's prior written permission.

May 14, 2003

UNIVERSITY OF ALBERTA

FACULTY OF GRADUATE STUDIES AND RESEARCH

The undersigned certify that they have read, and recommend to the Faculty of Graduate Studies and Research for acceptance, a thesis entitled **Use of Structured Packing as a Dualflow Tray in Distillation** submitted by **Jason Patrick Kachur** in partial fulfillment of the requirements for the degree of **Master of Science in Chemical Engineering**.

Dr. K. T. Chuang, Co-Supervisor

Mr. A. Afacan, Co-Supervisor

Dr. R. E. Hayes

Dr. S. A. Craik

May 12, 2003

ABSTRACT

Dualflow trays, or trays without downcomers, are a type of vapour-liquid contacting device used in mass transfer applications. This type of tray is known for having a higher capacity and lower pressure drop than conventional cross-flow trays.

In this study, a novel dualflow tray design is proposed. This new tray type makes use of a thin slice of structured packing and, as such, is named the structured packing tray (SP-tray). This tray type is compared to the commercially available and widely known dualflow sieve tray using hydraulic and mass transfer characteristics.

The SP-tray was found to have a higher capacity compared to the dualflow sieve tray. However, the stability of the SP-tray is strongly dependent on the liquid density of the system and liquid loading. While the SP-tray out-performs the dualflow sieve tray in high liquid density systems (ρ_L = 1000 kg/m^3) and operation at high L/V ratios, it appears to be susceptible to spraying in low liquid density systems (ρ_L=788 kg/m^3) and, as such, its capacity is decreased. It was found that the efficiency of the SP-tray remains fairly constant over a wide range of vapour loadings which demonstrates a high turndown ratio; whereas for the dualflow sieve tray, the efficiency is strongly dependent on the vapour loading.

Overall, it is the author's belief that the SP-tray is a superior tray when operated under the right conditions. Operation in distillation conditions using high liquid density systems and high liquid loadings as found in absorption columns are thought to be the optimal conditions for operation of the SP-tray. Based on the work presented in this thesis, further studies into the operation of the SP-tray are warranted.

DEDICATION

I would like to dedicate the completion of this thesis to my late grandparents; Mike and Milly Matychuk. The pride they displayed in me as their grandson was an inspiration to continue to excel in my studies and to show pride in every one of my accomplishments. Vichnaya Pam'yat!

ACKNOWLEDGEMENTS

I would like to thank Dr. Karl T. Chuang for his extremely valuable insight into my project. The many discussions that we had were both challenging and rewarding. I am truly humbled to have worked with one of the most noted experts in the field of distillation; a true guru. Not only did he teach me lessons pertaining to this project but also practical life lessons in order to make me a better engineer.

My utmost respect and admiration go toward Mr. Artin Afacan, a man with such patience and understanding of the hurdles faced in research. Thanks go to him for putting up with my endless questions and impatient attitude. Always willing to put his other work aside and lend an ear, he is a true friend.

Most of all, though, my thanks goes to my family; my mother, Beverley, my father, Steve, and my sister, Sarah. Without their continuous and never fading support this thesis would have seemed a lot harder. Their inspiration to be the best that I could be was the most influential driving factor in my advancement towards this graduate degree. I will never forget what they have done for me over the years.

TABLE OF CONTENTS

CHAPTER		PAGE
1.	**INTRODUCTION**	1
1.1	DUALFLOW TRAYS	1
1.2	DUALFLOW SEIVE TRAYS	7
2.	**EXPERIMENTAL METHODS**	14
2.1	HYDRAULIC STUDY	17
2.2	EFFICIENCY STUDY	19
2.3	PHYSICAL PROPERTY DETERMINATION	21
3.	**RESULTS AND DISCUSSION**	23
3.1	TRAY HYDRAULICS	23
3.1.1	Dry Tray Pressure Drop	24
3.1.2	Dynamic Liquid Holdup and Loading Points	26
3.2	TRAY OPERATION	33
3.2.1	Operational Limits	33
3.2.2	Effect of L/V Ratio	43
3.2.3	Surface Tension Effects	45
3.2.4	Liquid Density and Viscosity Effects	47
3.3	TRAY EFFICIENCY	56

3.4 HETP 61

3.5 TRAY MIXING 64

4. CONCLUSIONS AND RECOMMENDATIONS 66

5. LIST OF REFERENCES 68

APPENDIX A: EXPERIMENTAL DATA 74

APPENDIX B: ADDITIONAL FIGURES 89

APPENDIX C: SAMPLE CALCULATIONS 100

LIST OF TABLES

TABLE **PAGE**

2.1 Geometric tray parameters 14

2.2 Physical properties of the systems studied 22

LIST OF FIGURES

FIGURE		PAGE
1.1	Comparison between the flow patterns across both a cross-flow and dualflow tray	2
2.1	Photograph of an SP-tray	15
2.2	Photograph of a dualflow sieve tray	16
2.3	Schematic diagram of experimental setup for hydraulic studies	18
2.4	Schematic diagram of experimental setup for mass transfer studies	20
3.1	Comparison of dry tray pressure drop between varying thickness of packing	25
3.2	Dry tray pressure drop for Gempak AW7 structured packing	27
3.3	Dynamic liquid holdup in 76.2 mm of packing	29
3.4	Dynamic liquid holdup in 114.3 mm of packing	30
3.5	Dynamic liquid holdup in 254.0 mm of packing	31
3.6	Total pressure drop as a function of F-factor for two different liquid loadings at a packing thickness of 254.0 mm	32
3.7	Comparison of froth height between varying thickness of packing at a liquid flowrate of 49.7 $m^3/h \cdot m^2$	34
3.8	Comparison of total pressure drop between varying thickness of packing at a liquid flowrate of 49.7 $m^3/h \cdot m^2$	35

3.9 Comparison of froth height between varying liquid flowrates at a packing thickness of 76.2 mm 37

3.10 Comparison of total pressure drop between varying liquid flowrates at a packing thickness of 76.2 mm 38

3.11 Comparison of froth height between varying thickness of packing in distillation conditions 40

3.12 Comparison of total pressure drop between varying thickness of packing in distillation conditions 41

3.13 Comparison of froth height between a SP-tray and a dualflow sieve tray at L/V=1 44

3.14 Comparison of the effect of physical properties on froth height between a SP-tray and a dualflow sieve tray at L/V=1 for different systems 46

3.15 Effect of surface tension on froth height at L/V=1 48

3.16 Comparison of the effect of system properties on froth height for a dualflow sieve tray (36.1 % open hole area) 49

3.17 Comparison of the effect of system properties on total pressure drop for a dualflow sieve tray (36.1 % open hole area) 50

3.18 Comparison of the effect of system properties on froth height for a 76.2 mm thick SP-tray 52

3.19 Comparison of the effect of system properties on total pressure drop for a 76.2 mm thick SP-tray 53

3.20 Comparison of measured and predicted froth heights using published correlations at L/V=1 for a dualflow sieve tray (36.1 % open hole area) 55

3.21 Comparison of Murphree tray efficiency between varying thickness of packing 59

3.22 Comparison of HETP values between varying thickness of packing..... 63

NOMENCLATURE

d	Tray hole diameter, mm
E_{MV}	Murphree tray efficiency, fractional
E_O	Overall column efficiency, fractional
g	Gravitational constant, m/s^2
HETP	Height equivalent to a theoretical plate, m
h_f	Froth height, m
h_L	Equivalent clear liquid height, m
H_{OG}	Overall height of a transfer unit, m
L	Liquid flowrate, $kmol/m^2 \cdot h$
m	Slope of the equilibrium line
M_L	Liquid molar mass, kg/kmol
N_A	Number of actual stages
N_T	Number of theoretical stages
T	Tray thickness, mm
U_S	Vapour velocity based on active area, m/s
V	Vapour flowrate, $kmol/m^2 \cdot h$
x	Liquid mole fraction
x_B	Liquid mole fraction in bottoms
x_D	Liquid mole fraction in distillate
y	Vapour mole fraction
z	Height of packing, m

Greek Letters

α	Relative volatility
α_{avg}	Average relative volatility
α_B	Relative volatility at bottoms composition
α_D	Relative volatility at distillate composition
ε	Porosity of the vapour-liquid layer on the tray
λ	Ratio of slope of equilibrium line to operating line
ρ_{air}	Air density, kg/m^3
ρ_G	Vapour density, kg/m^3
ρ_L	Liquid density, kg/m^3
ϕ	Tray open hole area, fractional

Chapter 1

INTRODUCTION

Distillation and its related separation methods are undoubtedly the most predominant of the basic thermal process engineering operations (Billet, 1979). The design and behaviour of distillation columns are among the most studied subjects in chemical engineering (Ravagnani et al., 1990). Chemical plants commonly have between 50 to 90% of their capital investment in separations equipment (Wankat, 1988). Distillation is a unit operation that has been around for a long time and continues to be the primary method of separation in processing plants. The preeminence of distillation for the separation of fluid mixtures is not accidental, but fundamental, and therefore unlikely to be displaced (Kister, 1992).

1.1. DUALFLOW TRAYS

When the flow pattern across a fractionation tray is taken into account, two groups of trays can be distinguished (Van den Berg, 1957). The first group includes those designs which allow only one of the phases to pass predominantly through it (cross-flow trays). The second group does not favour one phase over the other but rather promotes both phases to flow counter-currently through it simultaneously. This second group provides the operating concept of the dualflow tray. A visual representation of the difference in flow patterns between the cross-flow and dualflow trays is shown in Figure 1.1.

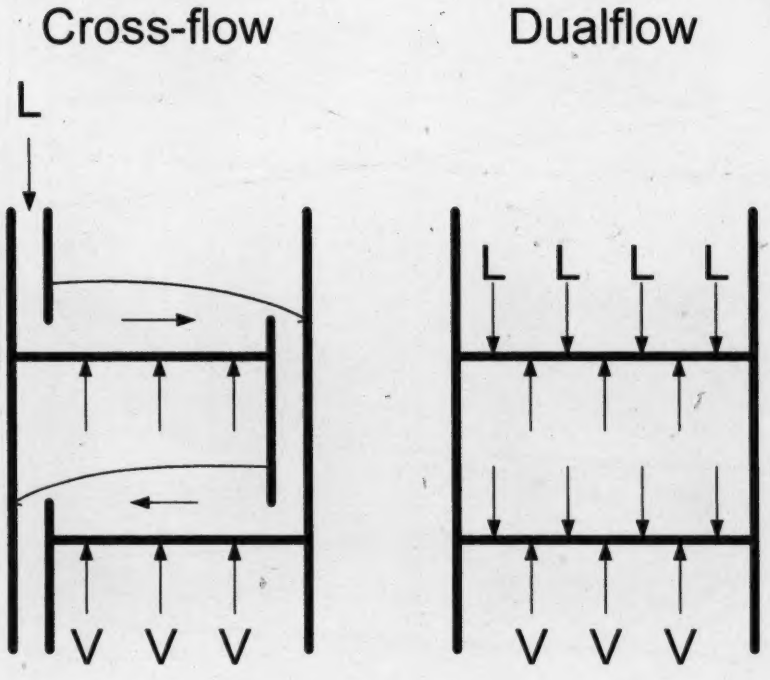

Figure 1.1. Comparison between the flow patterns across both a cross-flow and dualflow tray

The development of the dualflow tray principal began in the early 1950's. Around this time several designs for dualflow trays emerged which included the dualflow sieve tray, Kittel tray, Turbogrid tray and the Ripple tray. Other less commercial names for dualflow trays include self-cleaning trays, shower trays, drip trays, downcomerless trays or trays without downcomers. The most recent development in this area of research came from Stahl Gmbh in Germany in 1994 when they introduced the Dualflex tray (Billet, 1997). Each tray design has had its own unique geometry while retaining the counter-current flow profile. Variances in design have ranged from circular to rectangular holes, flat to corrugated plate decks and the incorporation of movable valves. While some designs promote a horizontal direction of liquid flow on the tray deck (Pfeiffenberger, 1953; Pollard, 1957), there are still no components specifically allocated for the passage of one phase over the other. The simplest design and most widely studied of all dualflow tray designs is the dualflow sieve tray. This tray was selected as the basis for comparison in this study due to the relatively large amount of literature available compared to other types of dualflow trays, the simplicity of operation and its feature of being the most widely known type of dualflow tray commercially since other designs have not been heavily promoted in recent years (Sloley, 1999). While other types of dualflow trays are used commercially, key performance data is generally kept confidential within the patenting company. The Shell developed Turbogrid tray, for example, has not been used outside of Shell or former Shell facilities (Sloley, 1999) and extensive testing results have never been released (Garcia and Fair, 2002).

Owing to the simplistic nature of the dualflow tray's design, many advantages have been realized and exploited. Dualflow trays are the only alternative of all tray type contactors (Kreis et al., 1979). The main advantage comes from the downcomerless nature of the tray. This leads to an increased capacity over conventional cross-flow trays because the entire cross-sectional area of the column can be used for fluid flow (Billet, 1997; Furzer, 2000; Kister, 1992; Kreis et al., 1979; Mahendru and Hackl, 1979; Ravagnani et al., 1990; Rylek and Standart, 1964; Shell, 1954; Sloley, 1999; Van den Berg, 1957; Xu et al., 1994). As well, this increased usage of the cross-sectional area leads to a decrease in tray pressure drop because vapour velocities through the orifices are decreased compared to columns with downcomers at the same vapour loading (Kreis et al., 1979; Mahendru and Hackl, 1979; Ravagnani et al., 1990; Rylek and Standart, 1964; Shell, 1954; Solomakha and Planovskii, 1963; Van den Berg, 1957; Xu et al., 1994). As such, dualflow trays are an ideal candidate for retrofit situations where higher capacity trays are needed (Kister, 1992).

The uncomplicated nature of these column internals is evidenced in the cost of such columns. With an absence of downcomers to design and install as well as the tray itself being geometrically relatively simple, design and construction costs are among the lowest of all trayed column designs (Billet, 1979; Billet et al., 1969; Furzer, 2000; Garcia and Fair, 2002; Kister, 1992; Kreis et al., 1979; Mahendru and Hackl, 1979; Miyahara et al., 1990; Ravagnani et al., 1990; Rylek and Standart, 1964; Shell, 1954; Takahashi et al., 1986).

Given that each orifice can only pass either liquid or vapour at any one time, oscillations in phase flow between the liquid and vapour through the orifices are created (Weiland, 2001). This flow oscillation is what separates the dualflow tray from other tray types as being the only tray suitable for fouling or dirty services (Baird, 1999; Billet, 1997; Billet, 2001; Garcia and Fair, 2002; Kister, 1992; Kreis et al., 1979; Mahendru and Hackl, 1979; Ravagnani et al., 1990; Rylek and Standart, 1964; Shell, 1954; Van den Berg, 1957; Xu et al., 1994). The oscillations result in a turbulent environment in the orifices which in turn provide a self-cleaning action within each orifice to keep it free from fouling or deposits.

Unlike cross-flow trays, dualflow trays promote complete mixing on the tray deck. Radial concentration gradients in both the vapour and liquid phases can be neglected if no serious channeling of fluids occurs across the tray. Where froth heights exceeded 50 mm on dualflow sieve trays, composition gradients in the liquid phase were less than 5% across the tray (Xu et al., 1994). The absence of relatively stagnant areas on dualflow trays is important as it contributes to the prevention of solids buildup (Shell, 1956; Sloley, 1999).

With conventional cross-flow trays, an increasing vapour flowrate generally decreases tray efficiency. This is a result of a decrease in liquid holdup on the tray and a decrease in vapour phase residence time. As well, an increased splash-over rate into the outlet weir is encountered, which also contributes to a drop in efficiency. Dualflow trays, on the other hand, have an efficiency curve which increases with vapour loading (Billet, 1997; Garcia and Fair, 2002; Garner et al., 1957; Rylek and Standart, 1964; Xu et al., 1994). However, the efficiency of a dualflow tray eventually

reaches a peak as vapour loading increases and begins to decrease very rapidly. The rate of efficiency decrease is significantly higher than the rate of decrease for a cross-flow tray as the vapour loading is increased. This parabolic efficiency profile is a characteristic of the dualflow tray and is a result of an increased proneness to entrainment at high vapour loadings. This parabolic efficiency profile provides a narrow operating range in which the efficiency of the tray is acceptable and thus, the tray is used less generally than traditional cross-flow trays (Billet, 1997; Billet et al., 1969; Garcia and Fair, 2002; Kreis et al., 1979; Molokanov et al., 1980; Pollard, 1957). As such, dualflow trays are usually applied to situations where a high turndown ratio is not essential (Billet, 1979; Garcia and Fair, 2002; Kister, 1992).

One of the most important drawbacks associated with dualflow trays in general is the lack of design models that can enable reliable prediction of their performance (Garcia and Fair, 2002; Mahendru and Hackl, 1979; Ravagnani et al, 1990; Rylek and Standart, 1964; Sloley, 1999; Xu et al., 1994). As well, the severe sensitivity of the tray's efficiency to the column loading and the physical properties of the system being separated also contribute to the reluctance to utilize this type of tray (Xu et al., 1994).

The capability of various dualflow trays to operate under varying liquid to vapour ratios (L/V) has been studied in the past (Billet, 1997; Billet, 2001; Furzer, 2000; Shell, 1954; Solamakha and Planovskii, 1963). Specific studies undertaken on dualflow sieve trays have investigated L/V ranges from 0.5 to 7.5 in absorption conditions (Solomakha and Planovskii, 1963), 0.6 to 1.0 in distillation conditions (Ravagnani et al., 1990) and 0.3 to 8.5 in air-aqueous solution conditions (Mahendru and Hackl, 1979). As such, it can be seen that dualflow trays are capable of operating

under extreme liquid loadings. As well, it has been shown that the stable operating range of a dualflow tray increases with increasing liquid load (Takahashi et al., 1986). Tray efficiencies have also appeared to increase toward higher L/V ratios (Billet, 1997; Billet, 2001; Shell, 1954).

1.2. DUALFLOW SIEVE TRAYS

To make a comparison with dualflow sieve trays, specific attributes associated with the dualflow sieve tray are investigated. These include the tray hydraulics, tray efficiencies, effect of tray geometry and areas for improvement with the current design.

Owing to the relative reluctance of industry to incorporate the use of dualflow sieve trays into their operation (Rylek and Standart, 1964), very little research has been performed on the hydraulic characteristics and the efficiency of this type of tray compared to the vast amount of open literature pertaining to traditional cross-flow trays. The majority of the past work has been on the hydraulics in particular of dualflow trays, although some authors have dealt with both hydraulics and mass transfer (Furzer, 2000; Furzer, 2001; Garcia and Fair, 2002; Mahendru and Hackl, 1979; Ravagnani et al., 1990; Sharma and Gupta, 1967; Solomakha and Planovskii, 1963; Steiner and Standart, 1967; Takahashi et al., 1986; Weiland, 2001; Xu et al., 1994).

Unlike tray hydraulics, efficiency studies are much more laborious and difficult to undertake. As such, fewer research efforts have been undertaken to shed light on the mass transfer processes that occur on dualflow sieve trays. Although

some mass transfer studies performed to date have focused on distillation (Garcia and Fair, 2002; Xu et al., 1994), the majority of open literature has been done in absorption applications (Billet, 1997; Miyahara et al., 1990; Sharma and Gupta, 1967; Solomakha and Planovskii, 1963). The most recent and by far most thorough work on the hydraulics and efficiency of dualflow sieve trays was done by Garcia and Fair (2002). The authors make use of recent data released by Fractionation Research Incorporated (FRI) which represents a vast number of systems and column configurations. The data are used to develop models for predicting both the hydraulic characteristics and mass transfer performance of dualflow sieve trays.

The unstable nature associated with dualflow sieve trays is reflected in their notoriously low efficiencies compared to traditional cross-flow trays. One reason for this comes from the existence of segmented zones of liquid dumping (Weiland, 2001). Clusters of holes tend to dump liquid while the remaining holes pass vapour. These segmented regions of dumping tend to align vertically from one tray to the next which promotes column-wide bypassing. While these clusters do move about the tray randomly, they still promote severe bypassing on the tray. As well, the tray's affinity for maldistribution is greatly amplified if the trays are even slightly off-level (Kister, 1992; Weiland, 2001; Xu et al., 1994).

It has been concluded that the efficiency of dualflow sieve trays is dependant on three main factors; vapour/liquid loading, physical properties and the most important being tray open hole area (Xu et al., 1994). The physical properties which were most influential on the trays efficiency were the liquid density and surface tension. The liquid density affects the froth density and froth height thus impacting

the vapour-liquid contact time and interfacial area. Surface tension affects the froth stability and bubble size.

It has been found that the vapour superficial velocity is the most important parameter for the stable operation of dualflow sieve trays (Ravagnani et al., 1990). Unlike cross-flow trays, the amount of liquid holdup on dualflow trays is strongly dependent on the vapour flow rate (Van den Berg, 1957). Compared to traditional cross-flow trays, the effect of vapour loading results in a higher turbulence in the froth and a higher froth height which leads to a higher vapour-liquid contact time. However, there is a relatively short contact time between the two phases since the liquid can weep through the tray without significant phase contact (Billet, 1997). The flow path length on the dualflow tray is essentially zero. This further reduces tray efficiency compared to cross-flow trays (Sloley, 1999). The Dualflex tray attempts to alleviate the problem of phase bypassing on the tray by installing movable valves. As such, vapour flow is directed horizontally on the plate and intimate phase contact is promoted (Billet, 1997; Billet, 2001).

The existence of segmented regions also leads to poor froth qualities which is evidenced in the poor tray efficiency. However, they are a requirement for the dualflow tray to operate (Steiner and Standart, 1967). The poor froth quality can be seen visually on the tray as the froth is very unstable and uneven. Analysis on the froth structure has led to the conclusion that in regions where there exist segments of liquid dumping, the froth can become liquid-continuous while above the remaining vapour-active regions the froth becomes vapour-continuous (Weiland, 2001). As such, two different operational regimes can co-exist on each tray; namely a froth and

spray regime. This froth and spray regime can also be thought of as bubbling and jetting at a submerged orifice respectively (Miyahara et al., 1983; Miyahara and Takahashi, 1984; Payne and Prince, 1975; Payne and Prince, 1977). However, a conflicting view says that the complete spray regime does not appear in plate columns without downcomers because the simultaneous passage of gas and liquid through plate holes promotes bubbling and suppressed jetting at the hole (Miyahara et al., 1990). This difference in operating regimes leads to the establishment of froth density gradients on the tray. A quantitative analysis performed on dualflow trays by Weiland (2001) points out that the density difference between liquid and vapour-continuous regions is critically important to the operation of the dualflow tray. Previous work has also noted that as the vapour loading on the column is increased, the froth density decreases (Sharma and Gupta, 1967). Owing to continuous weeping of liquid from one tray to the next, additional interactions between the weeping liquid and the froth and spray from the tray below must be considered. This type of interaction is absent in cross-flow trays and the downflow of weeping liquid may result in a decreased froth height (Furzer, 2000; Furzer, 2001).

It has been observed that the froth tends to slosh around or form waves on the tray (Ravagnani et al., 1990; Rylek and Standart, 1964; Steiner and Standart, 1967) and, as such, large hydraulic gradients are promoted within the froth. This sloshing on the tray has also been described as churn flow since there is a recirculation of froth flow evidenced as oscillations traveling from wall to wall (Furzer, 2001). It has been noted that as the vapour-liquid loading on the column is increased, the waves become larger and more regular until finally the froth is regularly displaced from one side of

the column to the other (Steiner and Standart, 1967). An in-depth study of these reported waves has been conducted (Shoukry and Kolar, 1974; Shoukry et al., 1974). The authors point out that two different types of waves can occur. The first type includes a swaying of the froth from one side of the column to the other. The second type is characterized by a nodal circle which oscillates from the center of the tray to the column walls.

Tray geometry has been found to play an important role in the operation of dualflow trays; namely tray open hole area and hole diameter. It has been shown that the operating range of a dualflow sieve tray is decreased with increasing hole diameter (Mahendru and Hackl, 1979). As well, larger holes favour jetting (Payne and Prince, 1975; Payne and Prince, 1977). One key point that has been shown for a set open hole area is that the larger the holes, the higher is the efficiency but the higher the pressure drop (Garcia and Fair, 2002). It has also been stated that the choice of hole diameter is only a matter of the fouling tendency of the system (Kreis et al., 1979). Further studies have revealed that the stable operating range of the column is increased when tray open hole areas are highest since the behaviour of the trays are strongly affected by it (Ravagnani et al., 1990). However, it has been determined that higher open hole areas lead to reduced froth heights and thus reduced tray efficiencies (Xu et al., 1994). The mean froth density was found to be independent of the plate dimensions (Takahashi et al., 1974).

For trays to gain acceptance in industrial applications, tray efficiencies of 70% or greater are desirable (Billet, 1997). If problems with reduced stage efficiency and operating stability are solved, then the dualflow tray may achieve substantial

improvements over current choices (Sloley, 1999). It has been shown here that there are a number of areas for improvement on the design of dualflow trays. Any design which would allow for extreme liquid loadings would be evidenced in a higher turndown and efficiency. Due to the relative lack of open literature on the performance of dualflow trays, any contribution to this area would be of great value. Because of the relatively short contact time inherent with dualflow trays, any effort to increase this time would be beneficial. As well, any design which would promote intimate contact on the tray by vapour flow redirection would be evidenced by higher tray efficiencies. In order for liquid distribution to become more uniform, the froth on the tray must become more stable. As well, it has been shown that reducing the hole diameter and increasing the tray open hole area has had positive effects on the operational limits of dualflow trays.

In this study, a new type of dualflow tray is investigated. The tray itself is a thin slice of Koch-Glitsch Gempak AW7 structured packing. The choice of this structured packing tray (SP-tray) is a result of its inherently low pressure drop due to its high internal void fraction of 97.8%. Since the open hole area of a dualflow sieve tray is limited to approximately 40% to maintain the integrity of the structure, it is hoped that this high void fraction would be equivalent to open hole area's far in excess of 40%. Additionally, the high void fraction would contribute to the tray's ability to operate under extreme liquid loadings, such as in absorption columns where the liquid flow rates are much higher than that of the vapour phase. It is also believed that the addition of the vapour-liquid contact time within the SP-tray itself would greatly increase the efficiency of such a tray compared to all other types of dualflow trays

which only promote mass transfer within the froth on the surface of the tray. In the following chapters, an in-depth study into the operation of the SP-tray is undertaken. Efforts will be made to demonstrate that the SP-tray attempts to resolve the above mentioned areas for improvement and thus is superior to current dualflow sieve tray technology.

Chapter 2

EXPERIMENTAL METHODS

For a detailed evaluation of both the hydraulic and efficiency characteristics, two separate experimental setups were required. Hydraulic studies were performed in an air/water column to obtain froth height and pressure drop data. Efficiency studies were performed in a distillation column which provided mass transfer characteristics. Detailed information on the type of trays used in both setups can be seen in Table 2.1. Photographs of an SP-tray and dualflow sieve tray are shown in Figures 2.1 and 2.2, respectively.

Table 2.1. Geometric tray parameters

	Gempak AW7 SP-Tray	Dualflow Sieve Tray
Crimp Height (mm)	7.0	-
Channel Base (mm)	26.4	-
Side of Corrugation (mm)	14.9	-
Void Fraction (-)	0.978	-
Surface Area (m^2/m^3)	345	-
Channel Angle (deg)	45	-
Tray Diameter (mm)	304.8	304.8
Tray Thickness (mm)	38.1-254.0	2.5
Hole Diameter (mm)	-	12.7
Open Hole Area (%)	-	36.1

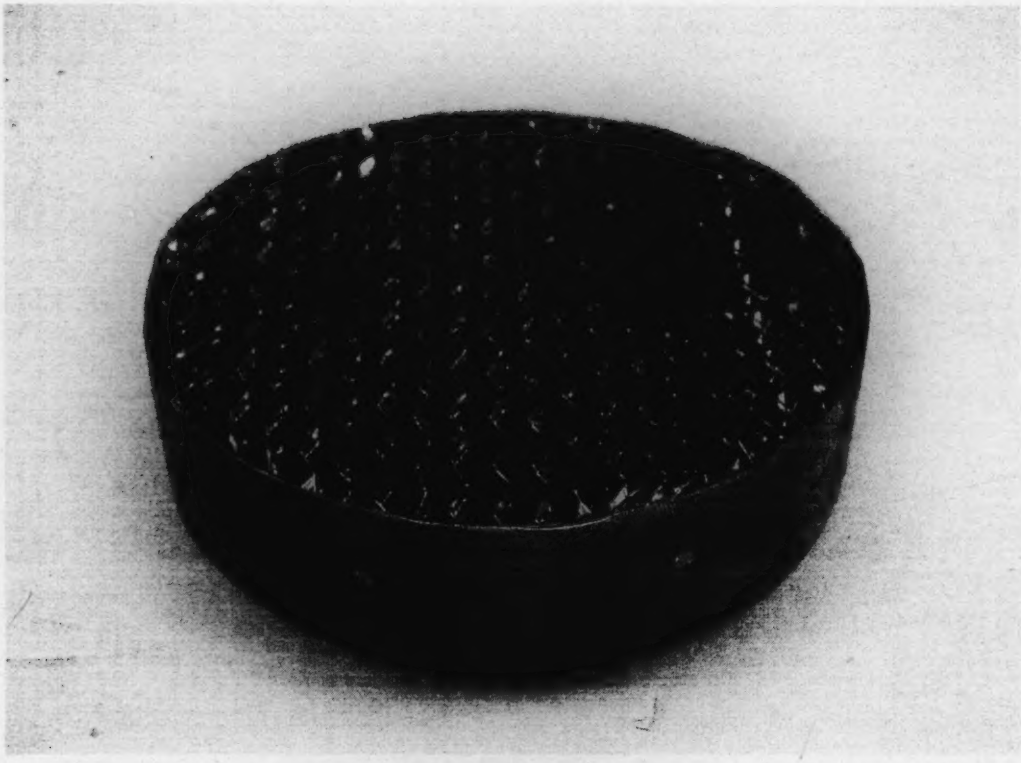

Figure 2.1. Photograph of an SP-tray

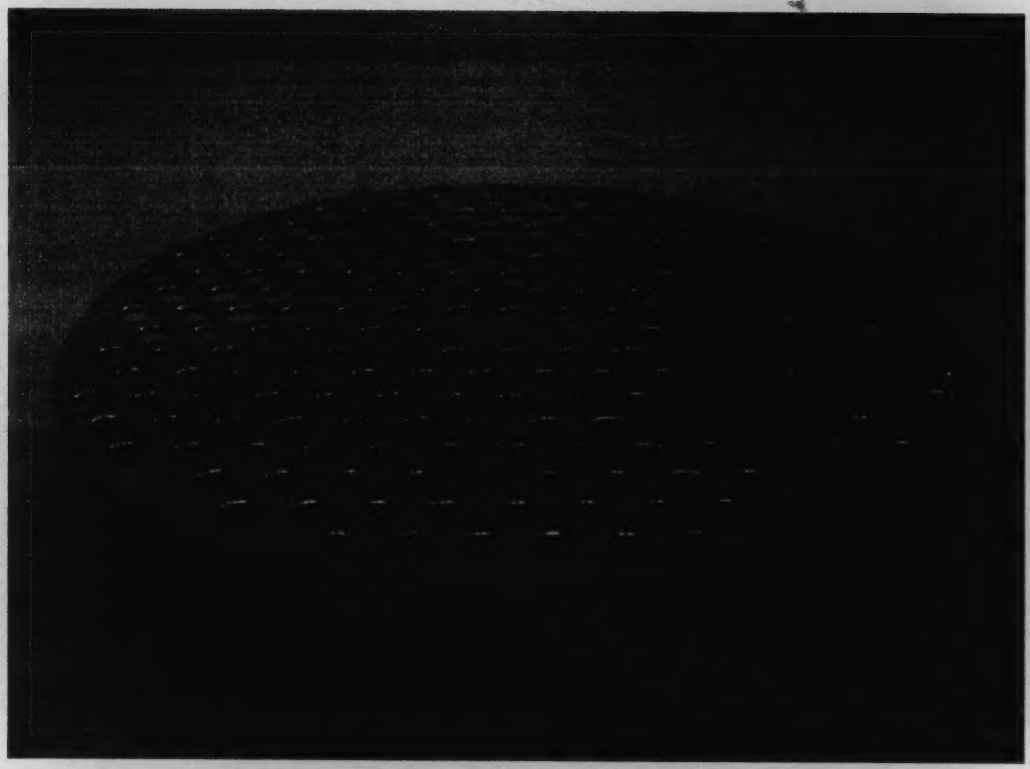

Figure 2.2. Photograph of a dualflow sieve tray

2.1. HYDRAULIC STUDY

Hydraulic characteristics of both the SP-tray and dualflow sieve tray were evaluated in a 304.8 mm diameter air/water column made of Plexiglas™. A schematic diagram of the equipment used is given in Figure 2.3. The working fluids of water, Isopar™-M and surfactant-water were used with air to study the effects of fluid physical properties on tray performance. The air was provided by a positive displacement blower. The water was recirculated using a pump from the holding tank. The Isopar™-M solvent was obtained from Esso. The effect of surface tension was studied by adding Electrasol dishwasher detergent tablets to the air/water system to lower the surface tension and minimize foaming. Flowrates of the air and liquid were measured using a hot-wire anemometer and rotameter, respectively. Pressure drop measurements were obtained using a Dwyer model 400 inclined manometer. A centre-to-centre tray spacing of 457 mm was used. Since the thickness of the SP-tray was varied, the actual tray spacing can be calculated by subtracting the tray thickness from the centre-to-centre tray spacing. Three trays were used in obtaining the hydraulic data. The top and bottom trays were 38.1 mm sections of Koch-Glitsch Gempak AW12 structured packing. This coarser packing, compared to the AW7 test tray, acted as a distributor for both the air and liquid while, due to an increased void fraction, did not affect the operation of the centre test tray. Tests using AW12 structured packing as an SP-tray were not possible due to the increased void fraction compared to the AW7 packing; the necessary liquid and vapour rates for the operation of this tray were unattainable with the existing experimental setup

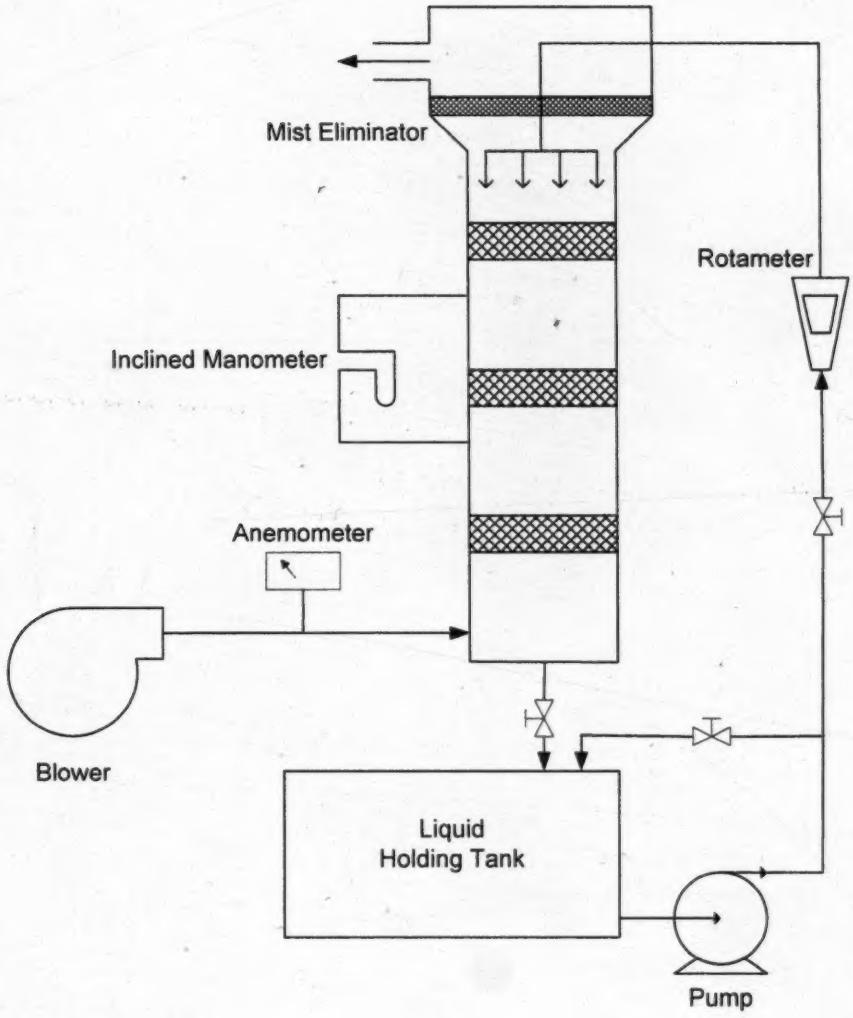

Figure 2.3. Schematic diagram of experimental setup for hydraulic studies

To simulate a broad range of operating conditions, both the air and liquid flowrates were varied. Liquid flowrates were varied from 12.5 to 49.7 $m^3/h \cdot m^2$ whereas, for the air, the flowrates varied from 0.7 to 5.8 $(kg/m)^{0.5}/s$. Changes were made to the flowrates and the system was allowed to reach steady state. The pressure drop across the test tray and a visual observation of the froth height were then recorded. Because froth height data were obtained visually, a maximum error of ±10 mm can be assumed. In order to verify the reproducibility of the data obtained, several identical experiments were conducted. Results of such experiments yielded results within ±5%. As well, in order to prove that no hysteresis effects were present, the vapour rate was both increased and decreased at a constant liquid loading.

2.2. EFFICIENCY STUDY

Mass transfer efficiencies were obtained from a 304.8 mm diameter distillation column operated under total reflux at ambient pressure using methanol/isopropanol. A detailed schematic diagram is shown in Figure 2.4. The 99.85% methanol and 99.0% isopropanol were supplied by Univar Canada Ltd. with product codes of LA1183 and LA2210, respectively. Both the steam to the reboiler and cooling water to the condenser were obtained from the building's utility lines. The column contained stainless steel sections with a Pyrex glass section on top of the first tray. A centre-to-centre tray spacing of 457 mm was used. Each section had two view ports installed at 90° to each other to allow visual observations between each tray. A total of four identical trays were installed in the column. The second tray from the top served as the test tray for pressure drop and froth height measurements. Mass transfer data

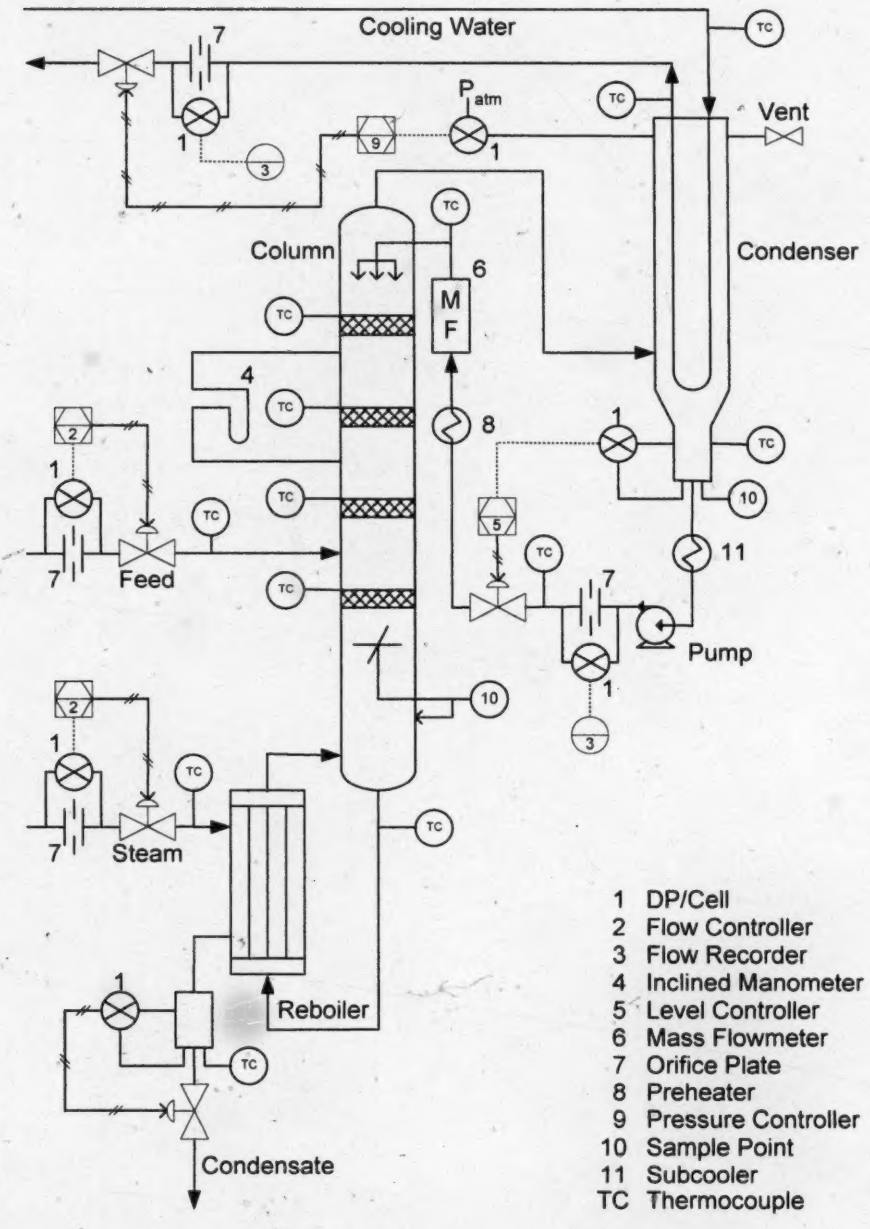

Figure 2.4. Schematic diagram of experimental setup for mass transfer studies

using a dualflow sieve tray were also obtained for comparison. The liquid reflux flowrate was measured using a Micro Motion Inc. model B50AF mass flowmeter.

To obtain varying vapour, and correspondingly liquid, flowrates, the steam pressure to the reboiler was adjusted. Vapour rates of 0.4 to 3.8 $(kg/m)^{0.5}/s$ were studied in the distillation column. After each steam flow setting, temperature and liquid flow profiles were monitored until they remained constant; which took approximately 45 minutes. At this point, the system is assumed to have reached steady state. Liquid samples were then taken from both the inlet to the first tray and the exit from the fourth tray and analyzed using a Hewlett Packard 5790A series gas chromatograph equipped with a Hewlett Packard 3392A integrator. Froth heights were recorded based on visual observation and pressure drop data were taken using a Dwyer model 400 inclined manometer. Accurate visual froth height measurements are more difficult to obtain in the distillation column because of the small view ports. As such, errors of ±20 mm can be assumed.

2.3. PHYSCIAL PROPERTY DETERMINATION

To determine the effects of physical properties, accurate data are required. The physical properties studied included the liquid surface tension, vapour/liquid densities and liquid viscosity. Data for the methanol/isopropanol system were taken from Wong (1993). Data for the air/water system were obtained from Young et al. (1997). Surface tension measurements for the water with surfactant and Isopar™-M systems were obtained using a Kruss model K12 processor tensiometer. The ring method was employed for such measurements. The viscosity of the Isopar™-M was measured

using a No. 100-1215 Cannon-Fenske Routine viscometer. The specific gravity of the Isopar™-M was determined using a hydrometer. A summary of the physical properties used is given in Table 2.2.

Table 2.2. Physical properties of the systems studied

System	Air/Water (T=20°C)	Air/Water/ Surfactant (T=20°C)	Air/Isopar™-M (T=20°C)	Methanol/ Isopropanol (saturation at x=0.65)
μ_L ($N \cdot s/m^2$)	1.00×10^{-3}	1.00×10^{-3}	2.87×10^{-3}	3.93×10^{-4}
ρ_L (kg/m^3)	998.2	998.2	788.0	733.5
ρ_G (kg/m^3)	1.20	1.20	1.20	1.49
σ (N/m)	7.28×10^{-2}	3.55×10^{-2}	2.46×10^{-2}	1.69×10^{-2}

Chapter 3

RESULTS AND DISCUSSION

To make an accurate comparison between the SP-tray and the commercially available dualflow sieve tray, specific operating attributes were investigated. These attributes included the tray pressure drops, froth heights and tray efficiencies. Tray pressure drop is important since the higher the pressure drop across a column, the more energy is required to push the vapour through the column. This is particularly important in vacuum distillation applications where tray pressure drop is a critical parameter; if the pressure drop is too high, the top of the column may be under vacuum whereas the bottom could be at or near atmospheric pressure. Froth heights are important in the operation and design of distillation columns. Tray spacings must be chosen taking into consideration the expected froth height on each tray. As well, froth heights impact the performance of each tray; namely through the vapour-liquid contact time and thus, tray efficiency. Physical properties such as surface tension, density and viscosity play a role in the froth structure and froth height. Finally, at the forefront of all operating attributes is the tray efficiency. Tray efficiency represents the trays ability to allow the vapour and liquid streams to approach equilibrium. Higher efficiencies result in better separation and lower capital and operating costs.

3.1. TRAY HYDRAULICS

As mentioned above, pressure drop and froth heights play a vital role in the operation of distillation trays. Presented below is an in-depth analysis of the hydraulic

performance of the SP-tray compared to a dualflow sieve tray (36.1% open hole area). Additional insight is given into the existence of a unique dynamic liquid holdup.

3.1.1. Dry Tray Pressure Drop

An important parameter in the design of a dualflow distillation column is the dry tray pressure drop. This is the pressure drop associated with vapour flow though the orifices in the tray without the presence of liquid. It is well known that larger holes and smaller open hole areas result in a greater pressure drop across a perforated plate. It was thought that the SP-tray would be superior to the dry tray pressure drop of a dualflow sieve tray because the openings of the SP-tray are small and the tray has a high void fraction. Dry tray pressure drop data were collected and are presented as a function of the F-factor in Figure 3.1. The F-factor is used because it represents the kinetic energy of the vapour stream flowing though the tray and is calculated using the following equation.

$$\text{F - factor} = U_s\sqrt{\rho_G} \tag{3.1}$$

Notice from Figure 3.1 how the dry tray pressure drop is approximately equivalent for both the 76.2 mm thick SP-tray and the dualflow sieve tray. This figure also shows that the 38.1 and 114.3 mm thick SP-trays have lower and higher pressure drops respectively, as would be expected. As such, no immediate benefits are realized by using the SP-tray. The decreased hole size and high void fraction are offset by the vapour having to travel through a tortuous path in the packing thus yielding a higher resistance to vapour flow. As such, the permeability of both the dualflow sieve tray and the 38.1 mm thick SP-tray is nearly identical. An interesting trend to note is how

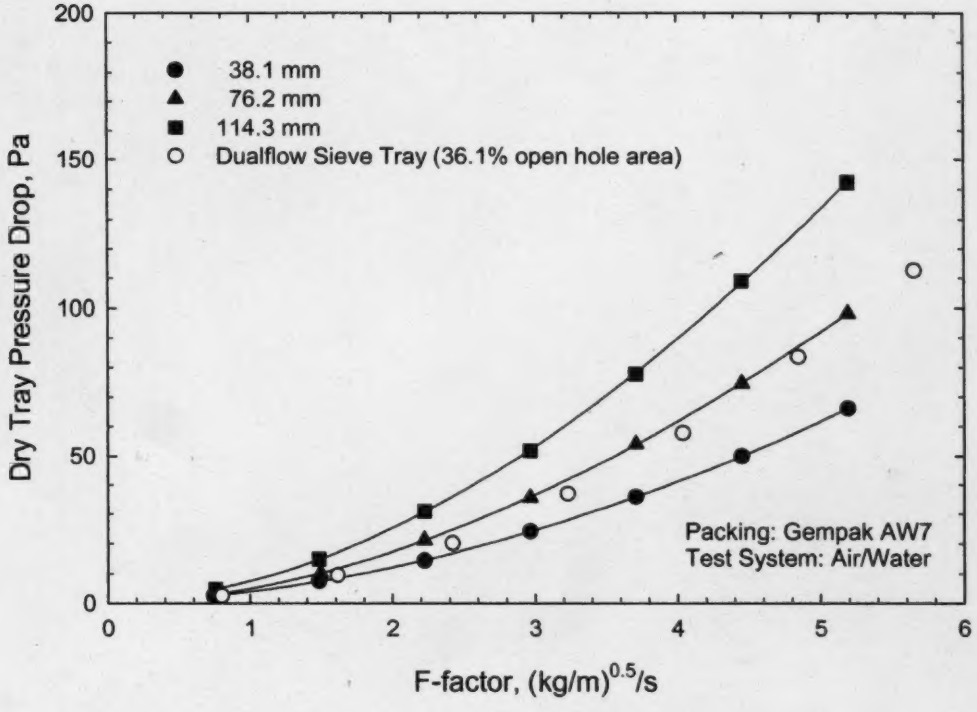

Figure 3.1. Comparison of dry tray pressure drop between varying thickness of packing

the pressure drop profile for the dualflow sieve tray mimics that of the SP-tray. This indicates that structured packing behaves very much like a perforated plate.

To verify the accuracy of the data collected between the three SP-trays, the dry tray pressure drop data were normalized using the tray thickness and are presented as a function of vapour loading using a log-log scale in Figure 3.2. As expected, the data collected from the three tray thicknesses lay along a common straight line. This verifies the accuracy of data taken between the three SP-trays.

3.1.2. Dynamic Liquid Holdup and Loading Points

A unique characteristic of the SP-tray is the trays' dynamic liquid holdup. Because the tray has an appreciable thickness, additional resistances associated with vapour flow will be encountered by the liquid film flow down through the packing. Studies were performed to provide information into the extent of this internal (dynamic) liquid holdup within the packing as a function of liquid and air flowrates. Liquid flowrates were kept constant and the vapour rate was increased. Initially, the vapour flow provides little resistance and the liquid flows freely down through the packing. At a certain loading point, the vapour provides enough resistance to cause the liquid film thickness to increase substantially. Finally, the entire depth of the packing is completely filled with liquid and thus, represents the flooding point; at this point, liquid is visible on the surface of the tray. Initially, data were collected from the three SP-trays investigated. However, data from the 38.1 mm thick SP-tray were discarded because the difference in vapour flow rates between the loading and flooding points was indistinguishable. As well, owing to the relatively thin nature of

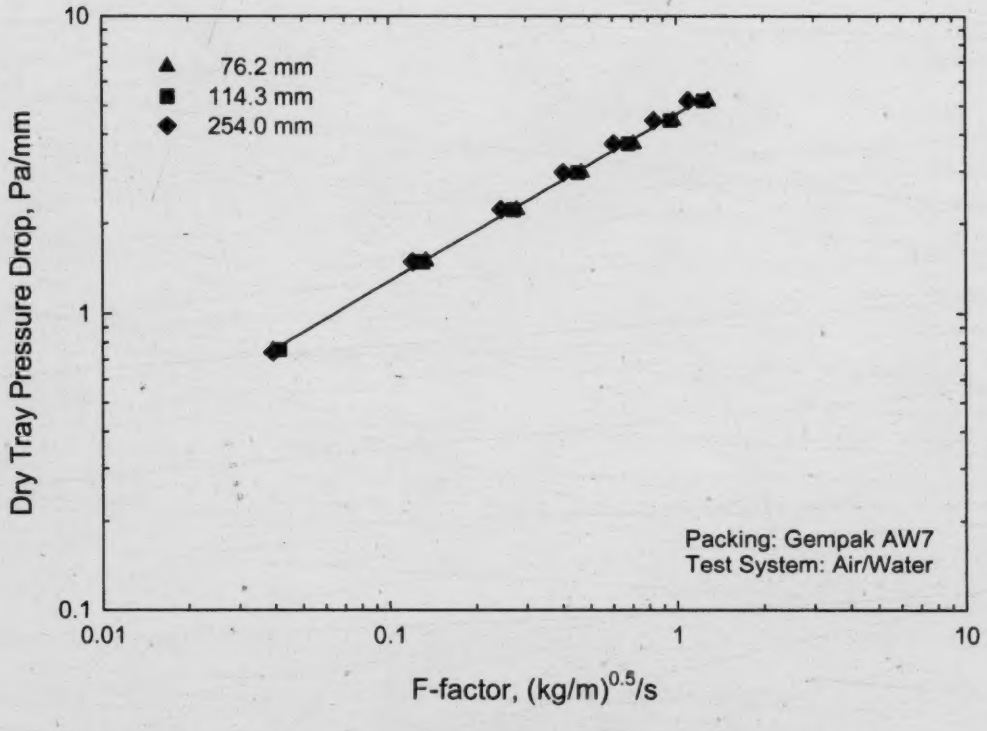

Figure 3.2. Dry tray pressure drop for Gempak AW7 structured packing

the 38.1 mm thick SP-tray, finding the exact point at which a surface froth was formed was inaccurate. The dynamic liquid holdup at different liquid loadings for the 76.2 and 114.3 mm thick SP-trays as a function of percent flood are given in Figures 3.3 and 3.4, respectively. Percent flood is calculated by taking the ratio of the F-factor to the F-factor at the dynamic liquid flood point. The dynamic liquid holdup is calculated by taking the total pressure drop across the tray and subtracting the dry tray pressure drop. From both figures, notice how initially there is little increase in the liquid holdup and then it increases substantially. This transition point corresponds to the loading point for that particular SP-tray. If the dynamic liquid holdup in the packing at the point of complete flood is normalized by the thickness of the packing, values of 2.88 and 2.94 Pa/mm are obtained for the 76.2 and 114.3 mm thick SP-trays, respectively. To verify the accuracy of these numbers, a 254.0 mm thick section of packing was also studied under the same conditions. These results are presented in Figure 3.5. By increasing the thickness of the packing, a more accurate value for the dynamic liquid holdup is obtained because the pressure drop at the flood point is normalized over a larger thickness. This resulted in a dynamic liquid holdup of 2.92 Pa/mm. This value lies between the previously obtained values with a maximum difference of 1.4% and was chosen as the most accurate value for the amount of liquid held within the packing at the flood point.

A comparison between the loading profiles at two different liquid rates as a function of vapour loading for 254.0 mm of packing is presented in Figure 3.6. Notice how two separate slopes exist for a given liquid flow rate. The first and lesser slope represents the region where there is no appreciable resistance to liquid flow through

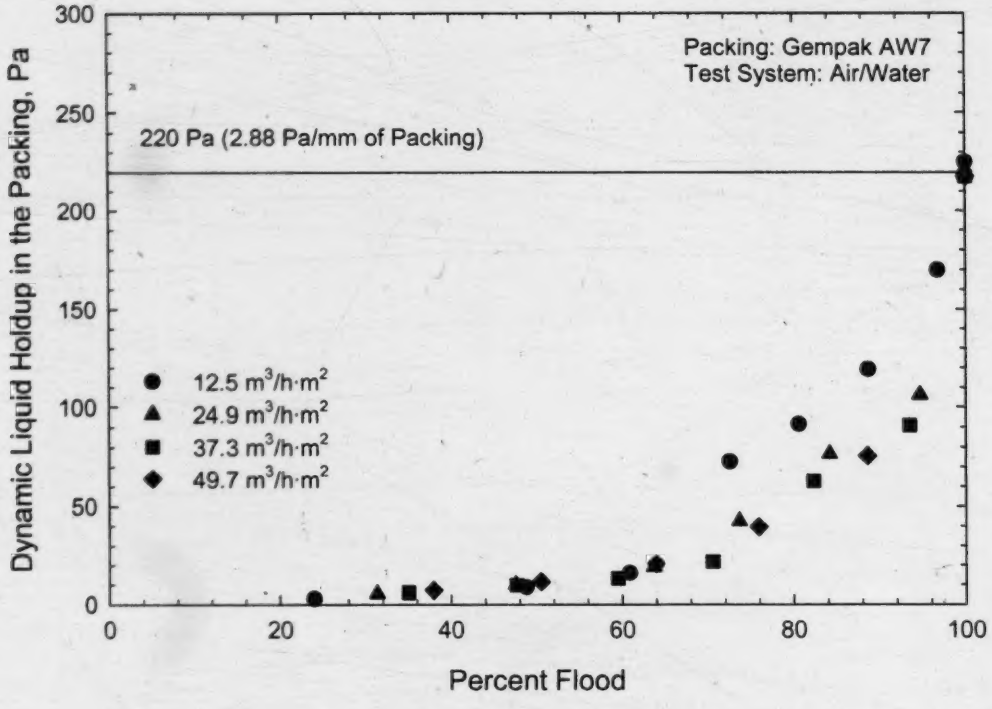

Figure 3.3. Dynamic liquid holdup in 76.2 mm of packing

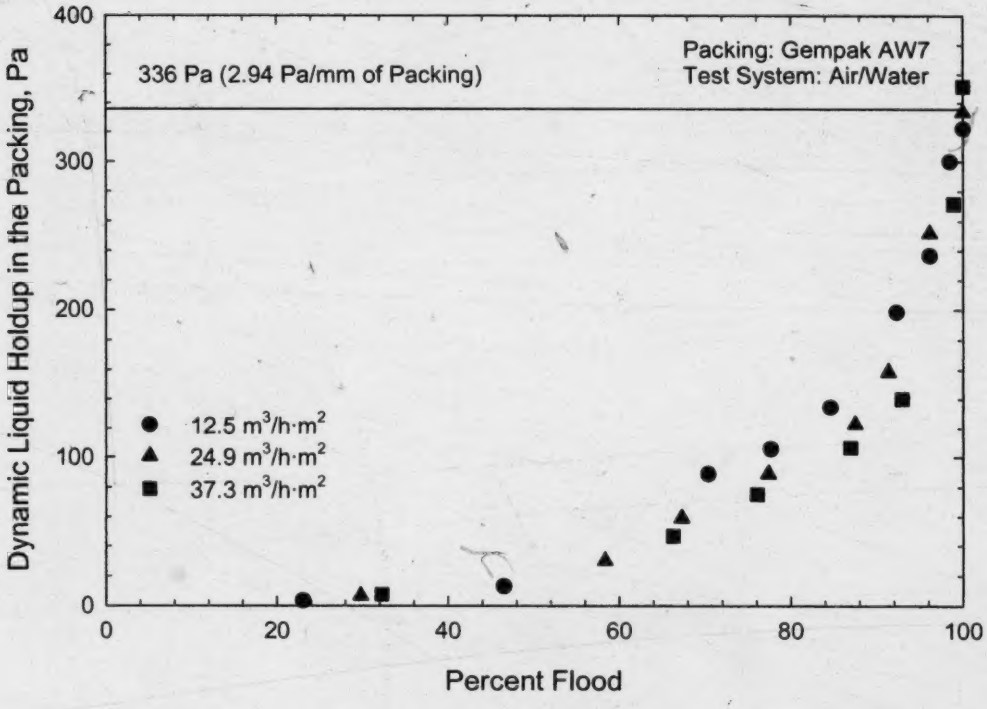

Figure 3.4. Dynamic liquid holdup in 114.3 mm of packing

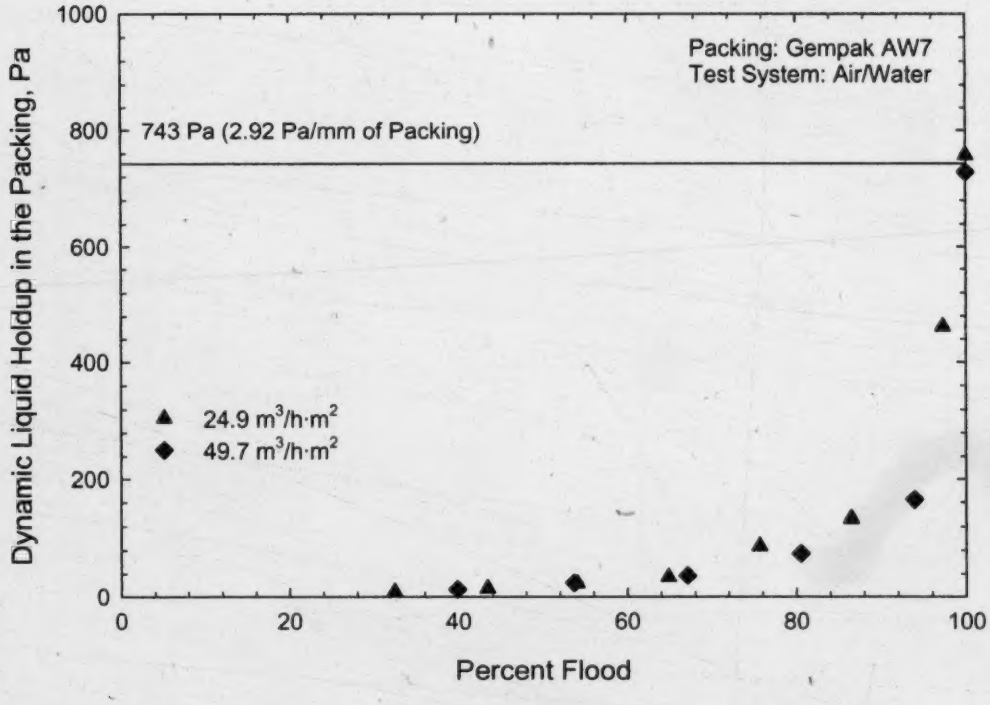

Figure 3.5. Dynamic liquid holdup in 254.0 mm of packing

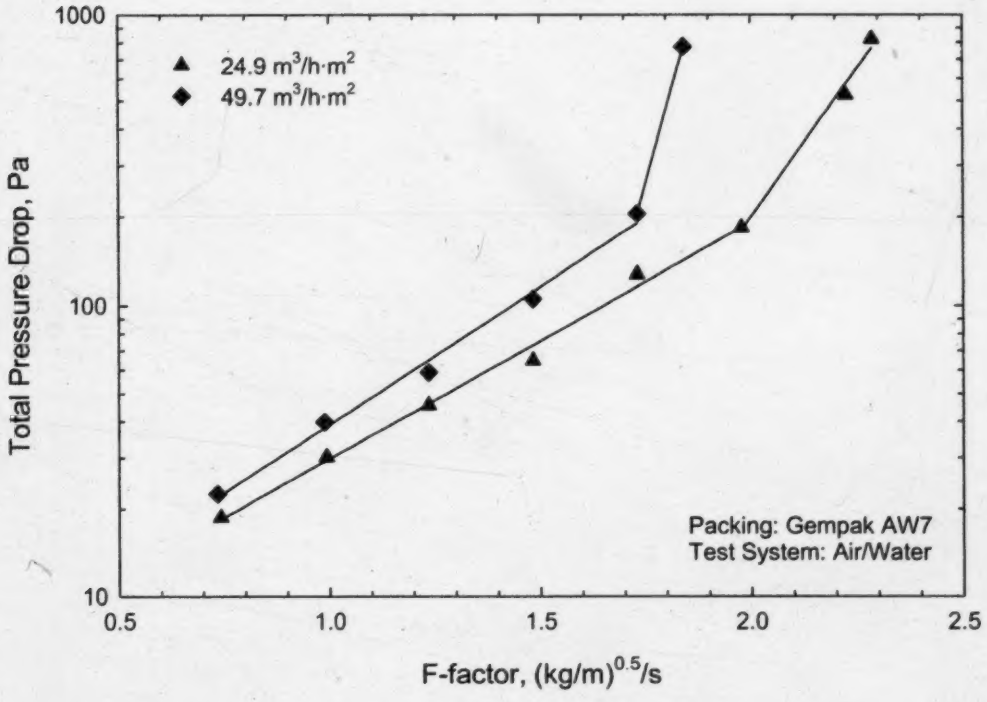

Figure 3.6. Total pressure drop as a function of F-factor for two different liquid loadings at a packing thickness of 254.0 mm

the packing. The second and higher slope represents the region from the loading point to the flooding point where the film thickness within the packing increases substantially. For each liquid rate, the point at the highest F-factor represents the dynamic liquid flood point. It should be noted that the pressure drop at the loading point where the slope changes remains relatively constant between the two liquid loadings.

3.2. TRAY OPERATION

The acceptability of a new tray design is strongly dependent on the tray's ability to handle a broad range of operating conditions. An increased tray capacity and turndown ratio are among the most important characteristics when considering tray performance. The turndown ratio is the ratio of the normal operating (or design) vapour throughput to the minimum allowable vapour throughput (Kister, 1992).

3.2.1. Operational Limits

The stable operating range of the SP-tray was studied over a wide range of operating conditions. These were obtained by varying the vapour flowrate at a fixed liquid flowrate. A comparison of the froth heights and pressure drop data between varying thickness of SP-trays and a dualflow sieve tray as a function of vapour loading can be seen in Figures 3.7 and 3.8, respectively. The froth height is defined as the highest point reached by the vapour-liquid dispersion on the tray. These curves represent the stable operating range from the initial formation of a froth on the tray to the point at which the column floods. It was found that the true flood point, or the

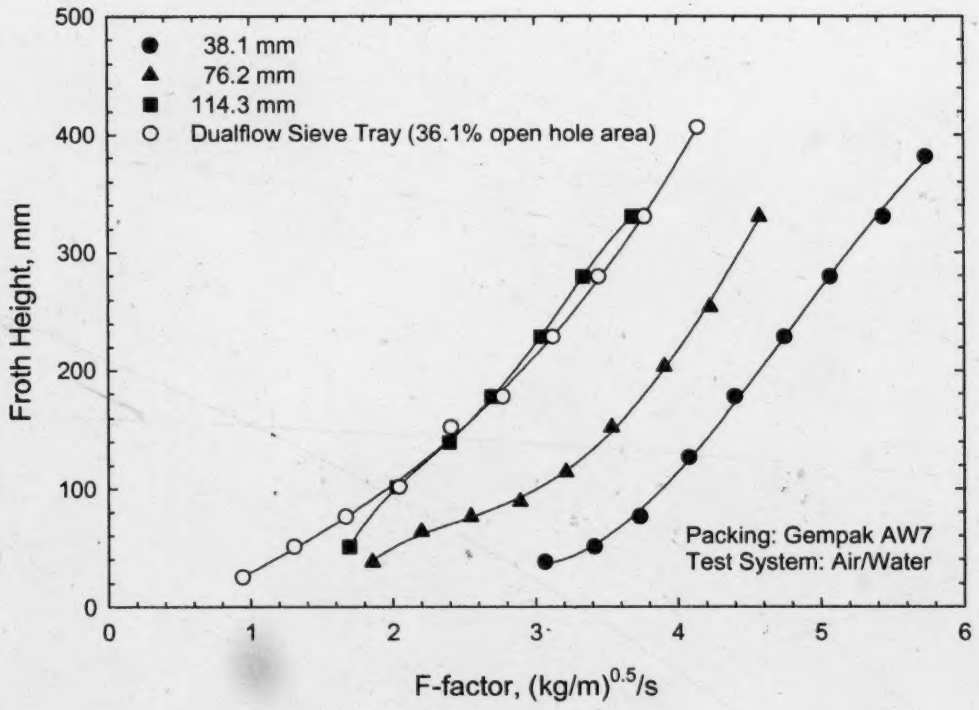

Figure 3.7. Comparison of froth height between varying thickness of packing at a liquid flowrate of 49.7 $m^3/h \cdot m^2$

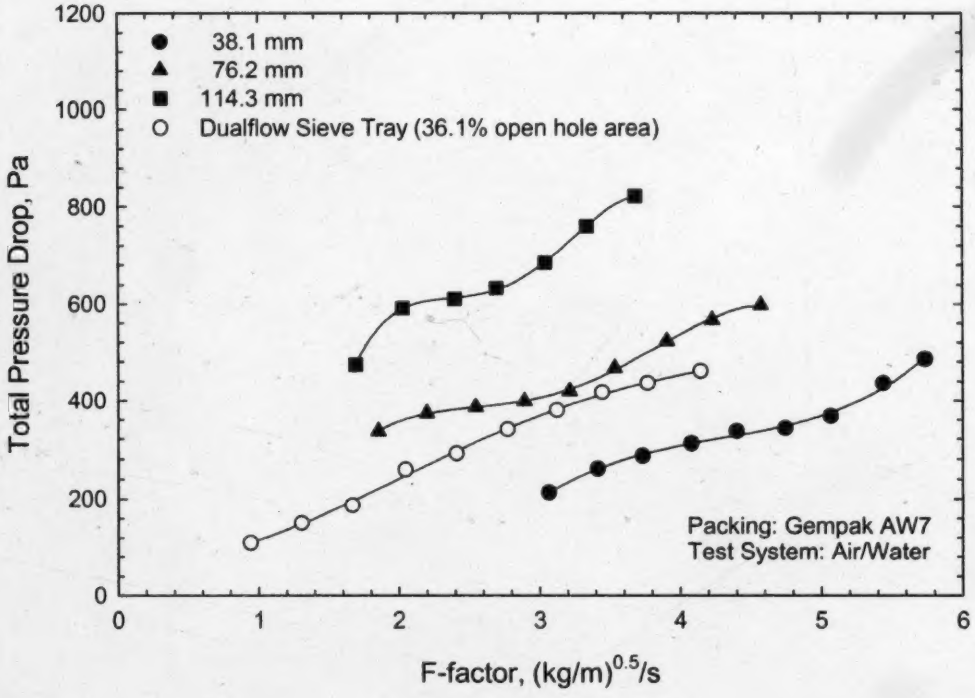

Figure 3.8. Comparison of total pressure drop between varying thickness of packing at a liquid flowrate of 49.7 $m^3/h \cdot m^2$

point at which no liquid flows down the column, could not be reached due to the extreme void fraction and therefore high capacity of the SP-tray. As such, the flood point is here defined as the point at which the froth height is equal to the tray spacing.

It is important to note from Figure 3.7 that an increase in capacity is realized by the use of the SP-tray over the dualflow sieve tray. While the dualflow sieve tray reaches a froth height of 300 mm at a minimum F-factor of 3.6 $(kg/m)^{0.5}/s$, F-factors as high as 5.2 $(kg/m)^{0.5}/s$ are attainable for the same froth height with the SP-trays. This represents an increase in capacity of 44%. The turndown ratios can be calculated from Figure 3.7 by dividing the F-factor at the flood point by the F-factor at the point of initial froth buildup. This results in a turndown ratio of 4.6 for the dualflow sieve tray. Turndown ratios for the 38.1, 76.2 and 114.3 mm thick SP-trays are 1.9, 2.6 and 2.2, respectively. This represents an average turndown ratio for the SP-tray of 2.2, a 52% decrease in turndown compared to the dualflow sieve tray. The results are due to the high void fraction present in the SP-tray.

Figure 3.8 reflects similar results to that of the dry tray pressure drop (Figure 3.1). The 76.2 mm thick SP-tray has a comparable pressure drop under liquid loading to that of the dualflow sieve tray. Additional figures representing a comparison to a dualflow sieve tray at a liquid loading of 24.9 $m^3/h \cdot m^2$ can be seen in Appendix B.

The effect of liquid loading on the operation of a 76.2 mm thick SP-tray as a function of vapour loading is shown in Figures 3.9 and 3.10. As expected, an increase in liquid loading is reflected by an overall decrease in the vapour rate needed to flood the column. As well, the resistance to vapour flow is increased by an increase in

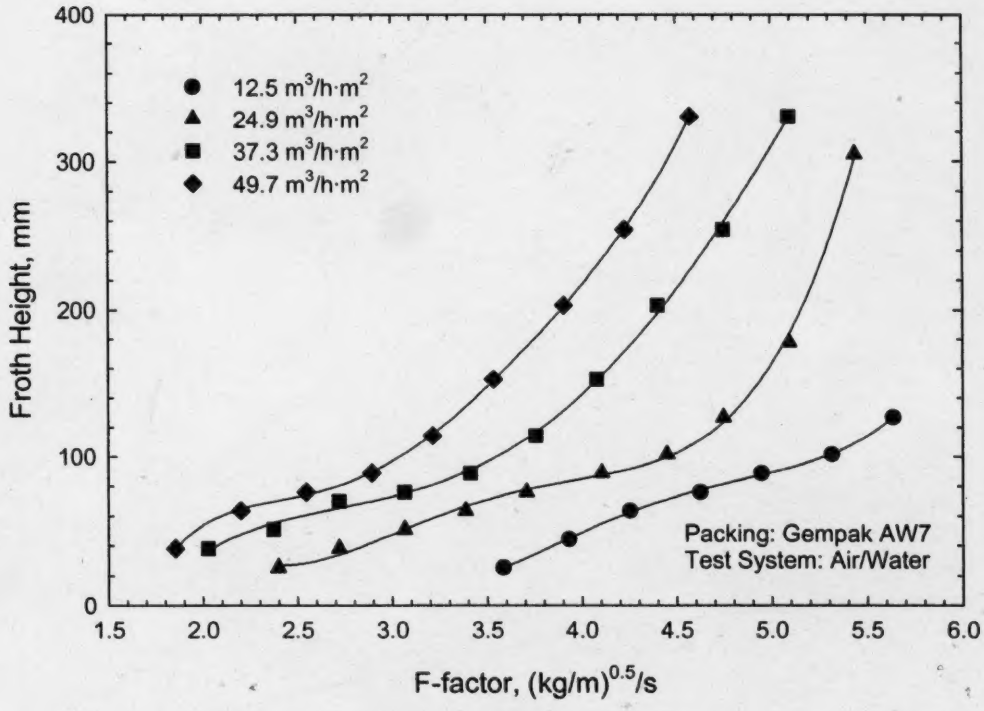

Figure 3.9. Comparison of froth height between varying liquid flowrates at a packing thickness of 76.2 mm

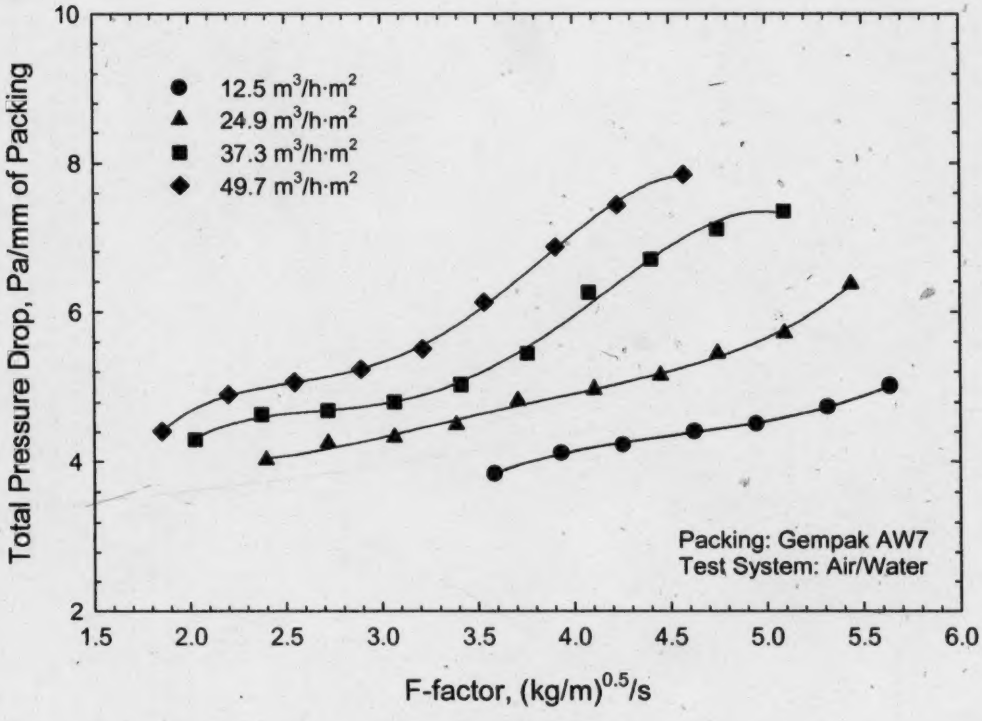

Figure 3.10. Comparison of total pressure drop between varying liquid flowrates at a packing thickness of 76.2 mm

liquid loading as evidenced by an increase in total pressure drop. Similar results were obtained for the 38.1 and 114.3 mm thick SP-trays and are presented in Appendix B.

Froth height data were also collected from the distillation column. A comparison between varying thickness of SP-trays and a dualflow sieve tray as a function of vapour loading is presented in Figure 3.11. The investigation of the 38.1 mm thick SP-tray in the air/water column yielded extremely unstable froths. This visual observation formed the basis for neglecting studies of this tray in distillation conditions. A discrepancy is observed with the operation of the SP-tray under distillation conditions compared to the air/water column. As can be seen in Figure 3.11, both SP-trays show a decrease in capacity of 17% compared to the dualflow sieve tray. As well, there is no distinct difference in the performance between the 76.2 and 114.3 mm thick SP-trays. The turndown ratio for the SP-tray is approximately 1.3 for the existence of a surface froth, significantly less that that from the air/water column.

The pressure drop profiles for the 76.2 and 114.3 mm thick SP-trays and dualflow sieve tray under distillation conditions are shown in Figure 3.12. It should be noted that Figures 3.11 and 3.12 represent data taken initially from very low vapour flow rates where there was no froth formation on the tray. Examining the data for the dualflow sieve tray, it can be seen that two operating zones exist. The first zone covers all vapour loadings up to an F-factor of approximately 1.3 $(kg/m)^{0.5}/s$. Up to this point there is no froth on the tray surface. At F-factors greater than 1.3 $(kg/m)^{0.5}/s$, a froth forms and the pressure drop rises correspondingly with the froth height.

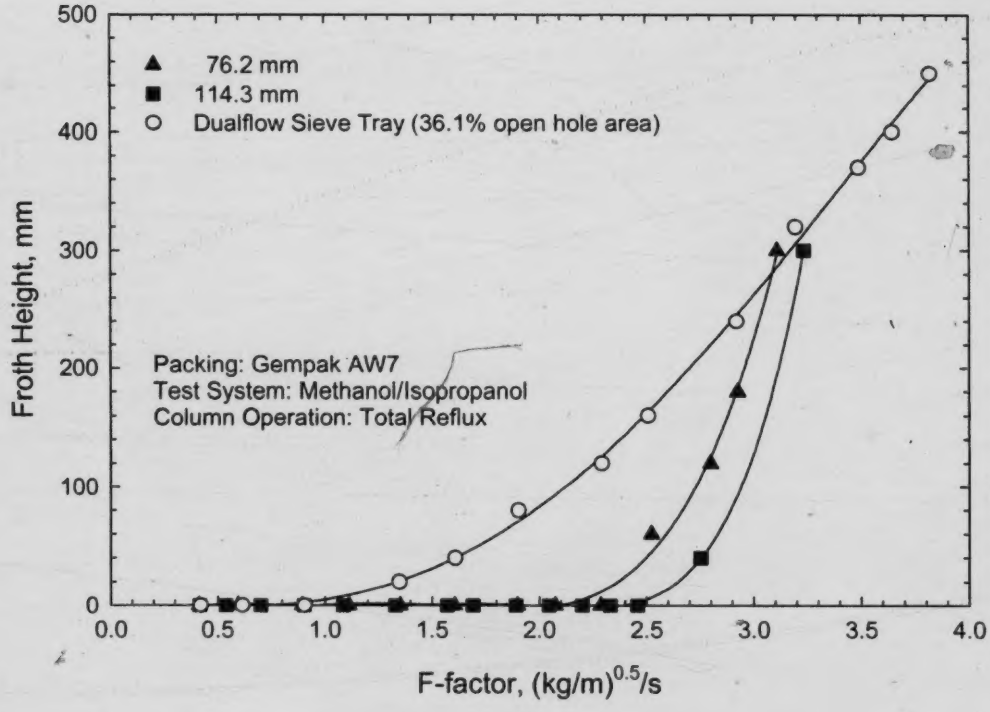

Figure 3.11. Comparison of froth height between varying thickness of packing in distillation conditions

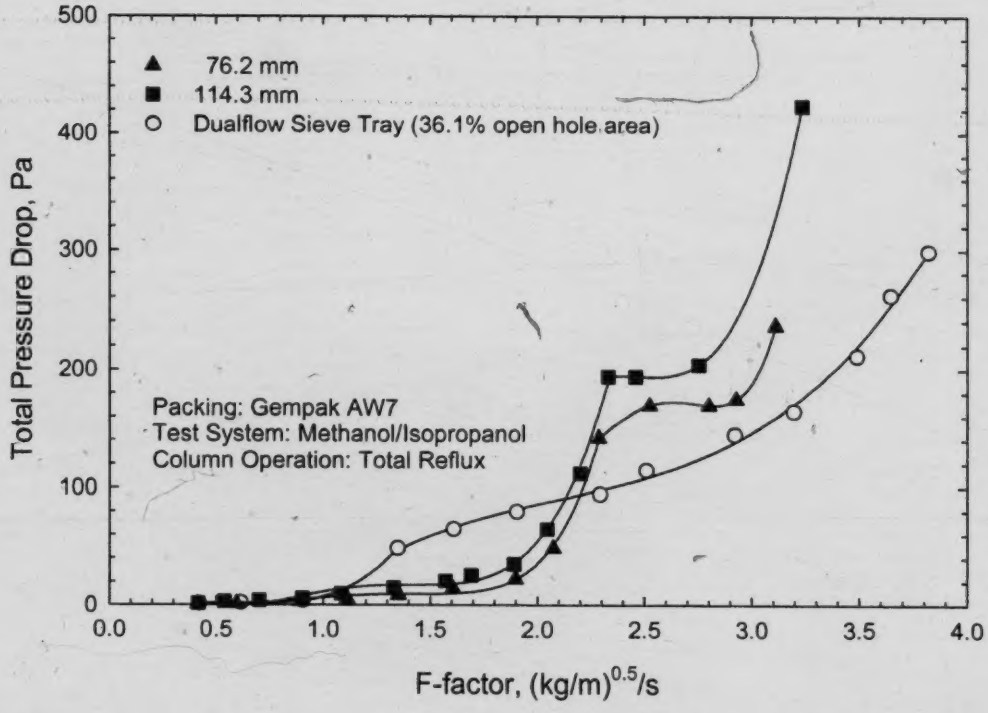

Figure 3.12. Comparison of total pressure drop between varying thickness of packing in distillation conditions

The data for the SP-trays show a unique pressure drop profile which can be explained by the existence of four operating zones. The first of these zones, classified as a "free-flow" zone (up to an F-factor of 1.9 $(kg/m)^{0.5}/s$), occurs when vapour flow rates are low and there is no increase in the liquid film thickness within the packing. This zone is characterized by the initial relatively flat pressure drop profile. The second zone, termed the "loading" zone (F-factor from 1.9 to 2.3 $(kg/m)^{0.5}/s$) occurs when the vapour flowrate is high enough to cause an increase in the liquid film thickness. This is evidenced by the sharp increase in pressure drop. The third operating zone is called the "blow-out" zone (F-factor from 2.3 to 2.8 $(kg/m)^{0.5}/s$). This occurs when the vapour rate is increased past the dynamic flood point of the tray. This region of operation causes the internal froth within the SP-tray, or dynamic liquid holdup, to move out of the tray and become an external froth on the surface of the tray. As such, nearly all of the liquid is blown out of the SP-tray and the tray essentially operates like a section of dry packing. This shift in froth position is evidenced by a relatively constant pressure drop while the vapour rate increases. The fourth and final operating zone has been named the "froth-dominated" zone (F-factors greater than 2.8 $(kg/m)^{0.5}/s$). This represents the region where the tray itself no longer contributes to a dynamic liquid holdup and the increase in pressure drop is dominated by a sharp increase in the froth height on the tray. The existence of these four operating zones has been verified by visual observation through the column view ports.

3.2.2. Effect of L/V Ratio

To explain the discrepancy between the increase in capacity observed in the air/water column and the decrease in capacity observed in the distillation column, several factors were considered. The first distinguishable difference between the two systems was the L/V ratio at which the two columns were operated. In the air/water column, the liquid flowrates were kept constant and the vapour rate was increased. L/V ratios, by weight, of 2.9 to 7.1 were encountered for the 76.2 mm thick SP-tray and 3.4 to 15.1 were obtained for the dualflow sieve tray. These values are much higher that that encountered in the distillation column which was operated under total reflux (L/V=1). It has been noted in open literature that the operating range of a dualflow tray has been seen to increase with an increase in liquid loading (Takahashi et al., 1986). It was believed that the high L/V ratios encountered in the air/water column could explain this increase in performance compared to that in the distillation column. In order to determine the cause of this discrepancy, specific comparisons between the dualflow sieve tray and the 76.2 mm thick SP-tray were undertaken. Additional experiments were carried out in the air/water column while maintaining L/V=1. Figure 3.13 shows a comparison between the 76.2 mm thick SP-tray and the dualflow sieve tray at L/V=1 as a function of vapour loading. A pressure drop comparison under the same conditions is given in Appendix B. As can be seen, even at L/V=1, the SP-tray still has a higher capacity than the dualflow sieve tray in the air/water column. As such, the observed discrepancy is not a result of the L/V ratio.

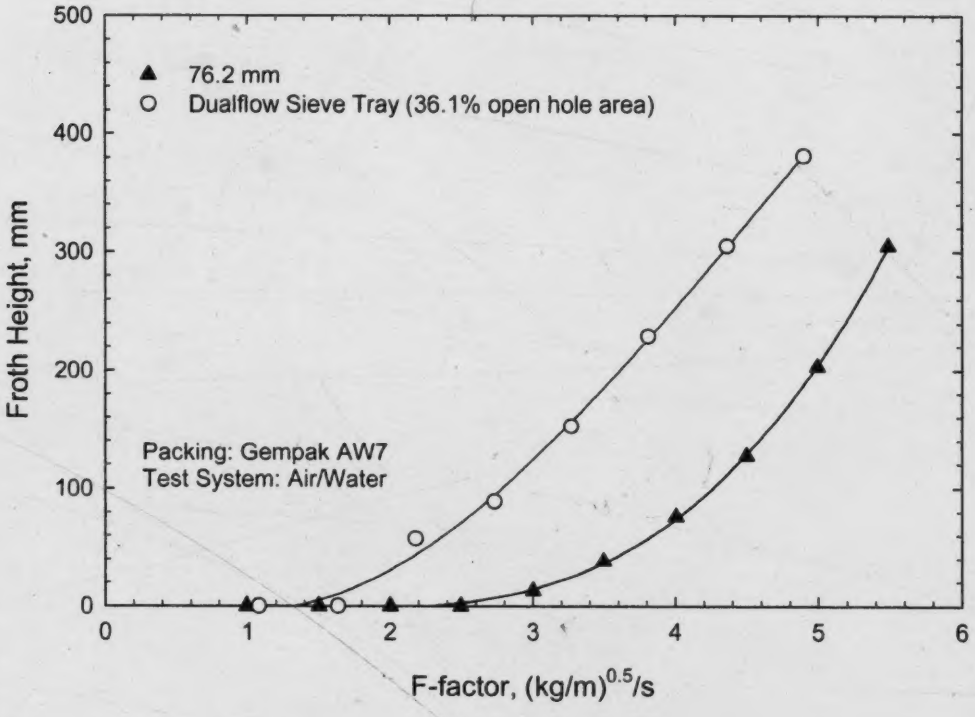

Figure 3.13. Comparison of froth height between a SP-tray and a dualflow sieve tray at L/V=1

3.2.3. Surface Tension Effects

With a new set of data consistent with the operating conditions found in the distillation column, L/V=1, it is possible to consider the effect of physical parameters on the operation of the tray. Froth height data from both the air/water column and the methanol/isopropanol distillation column for the 76.2 mm thick SP-tray and the dualflow sieve tray are compared and shown in Figure 3.14. The pressure drop data are given in Appendix B. Notice that for both the SP-tray and the dualflow sieve tray there is a shift in the operational capacity between the two systems. A decrease in capacity is observed in going from air/water to methanol/isopropanol. Even more pronounced is the shift in capacity for the SP-tray. To determine the causes of this shift, physical property differences in the systems must first be identified. Because the data are plotted as a function of the F-factor, differences in vapour densities can be neglected. This is because the vapour densities are already taken into account by normalizing the vapour stream using the kinetic energy. Large differences are noted in the viscosity, liquid density and the surface tension. To determine which physical property is most influential on this shift in capacity, the process of elimination was used. The first property studied was the effect of the surface tension. Lowering the surface tension of a liquid in a froth causes two main effects. First, the size of the bubbles is decreased. When a froth exists, there is a driving force to minimize the energy of the system. This energy is minimized by the coalescence of smaller bubbles into larger ones. However, a lowered surface tension decreases this drive to minimize energy and thus the bubbles remain smaller for longer periods of time. The second effect caused by a lowering of the surface tension is actually a result of the first one.

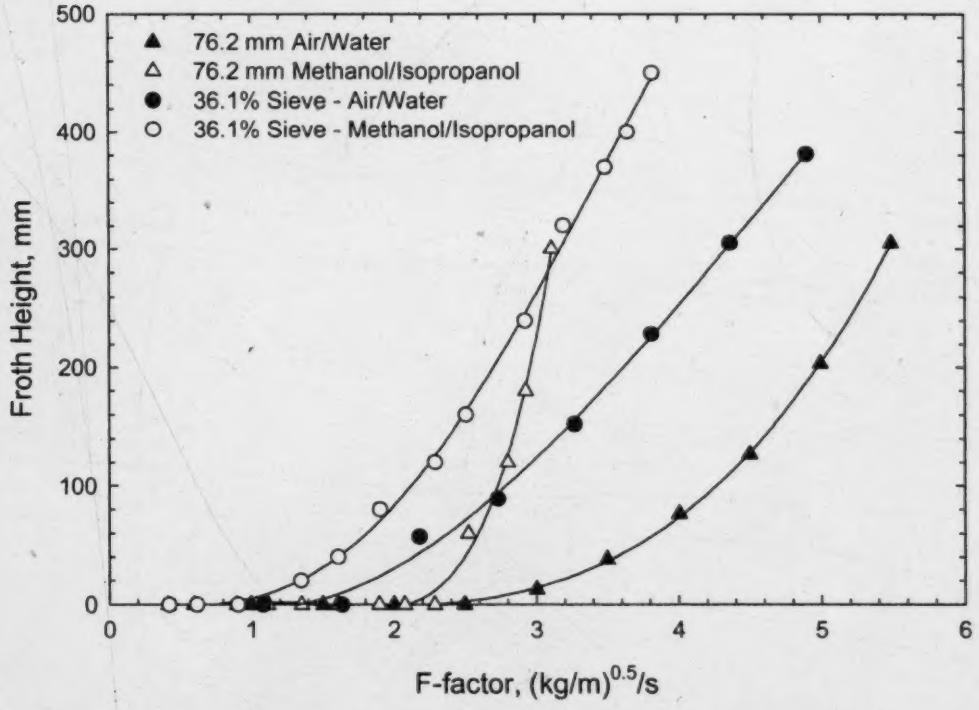

Figure 3.14. Comparison of the effect of physical properties on froth height between an SP-tray and a dualflow sieve tray at L/V=1 for different systems

By allowing the bubbles to remain smaller, the froth tends to become more stable because the bubbles do not coalesce as fast and the froth will not collapse down on itself as quickly. As such, lower surface tension systems tend to produce more stable froths with greater heights for a given F-factor. Dishwasher detergent tablets were added to the water to reduce the surface tension keeping the liquid density and viscosity constant. The surface tension of the water was lowered by approximately 51%. If the difference in surface tension was the cause of the shift in capacity this experiment would yield the same shift. The effect of surface tension on froth height for both the 76.2 mm thick SP-tray and the dualflow sieve tray can be seen in Figure 3.15 with pressure drop data given in Appendix B. Note how lowering the surface tension had no effect on the operational capacity of either tray. As such, the shift in capacity is not a result of the lower surface tension of the methanol/isopropanol system.

3.2.4. Liquid Density and Viscosity Effects

To determine which of the two remaining physical properties, namely liquid density and viscosity, were responsible for the shift in capacity, Isopar™-M solvent was used with air in the air/water column (see Table 2.2 for physical properties). Figures 3.16 and 3.17 show the effect of physical properties on the operation of the dualflow sieve tray as a function of vapour loading. Notice, from Figure 3.16, how the froth heights using Isopar™-M match extremely well with the results from the methanol/isopropanol system. Examining the physical properties between these two systems, it can be seen that the liquid densities are relatively similar. Although the

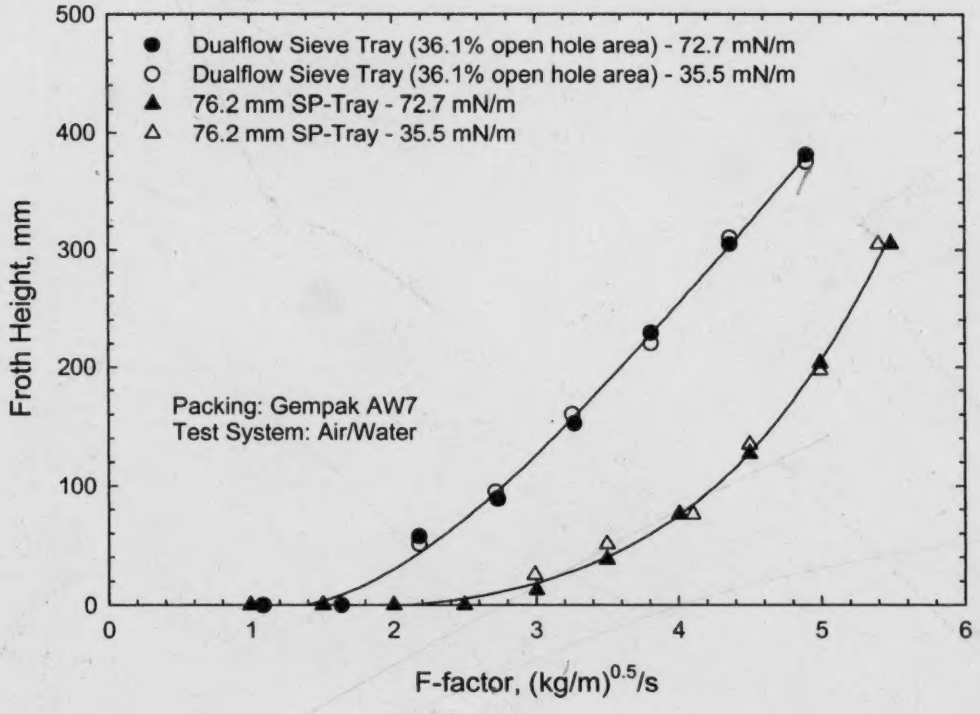

Figure 3.15. Effect of surface tension on froth height at L/V=1

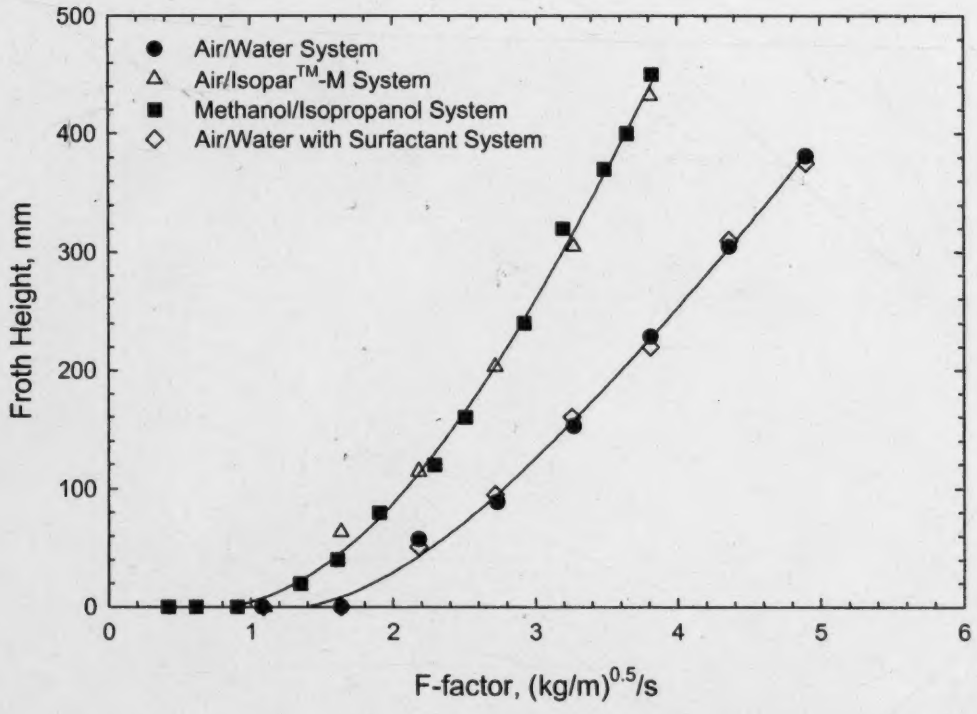

Figure 3.16. Comparison of the effect of system properties on froth height for a dualflow sieve tray (36.1% open hole area)

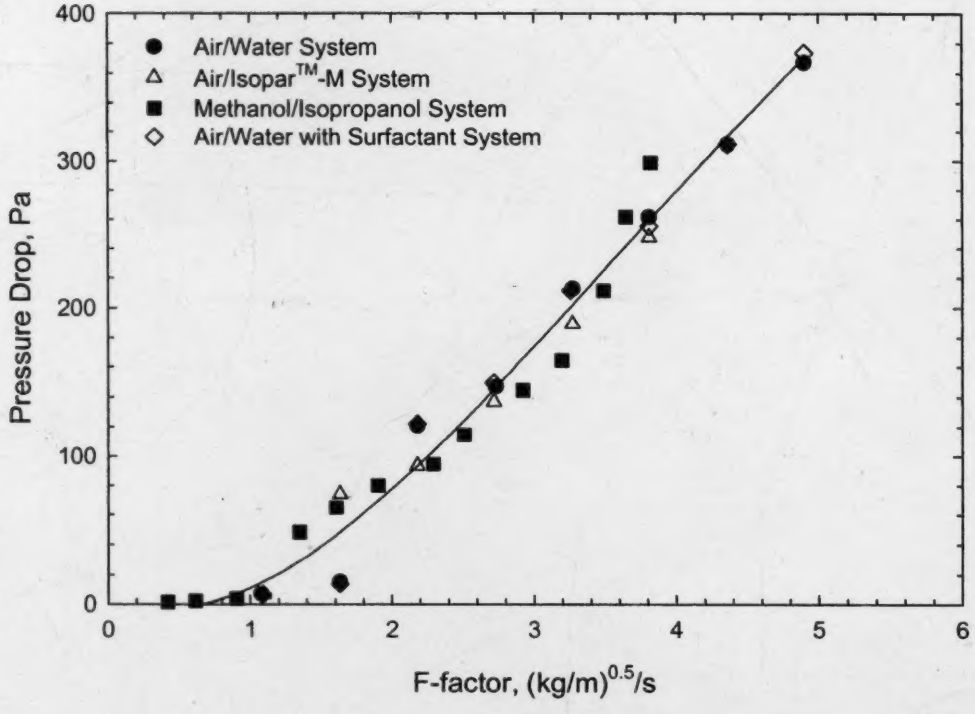

Figure 3.17. Comparison of the effect of system properties on total pressure drop for a dualflow sieve tray (36.1% open hole area)

surface tension does differ by approximately 46%, it can be neglected as this was not found to be a contributing factor (see Section 3.2.3). The only difference left is the liquid viscosity. The liquid viscosity of the Isopar™-M solvent is 7.3 times higher than that of the methanol/isopropanol system. As such, it can be concluded that the liquid viscosity has no observable effect on the froth height. Identical experiments were carried out using a 76.2 mm thick SP-tray with the results presented in Figures 3.18 and 3.19. The tests revealed the same results as those found for the dualflow sieve tray. Through the process of elimination it has been determined that the only physical parameter responsible for a change in froth height is the liquid density.

Through visual observations of all four systems in both the air/water and distillation columns, differences in the froth structure have also been seen. The operation of the dualflow sieve tray was observed to have a liquid continuous froth on the tray. This froth was observed to slosh around on the tray from wall to wall. However, the froth on the SP-tray was observed to be nearly vapour-continuous with no sloshing present. That is, the SP-tray appeared to operate at or near the spray regime at all times. As such, the previously reported froth heights could be thought of as spray heights. The spray height is defined as the height which the majority of the liquid droplets reach. This is a result of the extremely high open hole area associated with such a high void fraction. This spray regime appeared to be amplified with a decrease in liquid density. If it is the case that the SP-tray never forms an actual liquid continuous froth this would explain the dramatic decrease in capacity that was observed. At a fixed F-factor, the liquid droplets would weigh less and as such would be carried higher by the vapour. Based on the above presented information, it is the

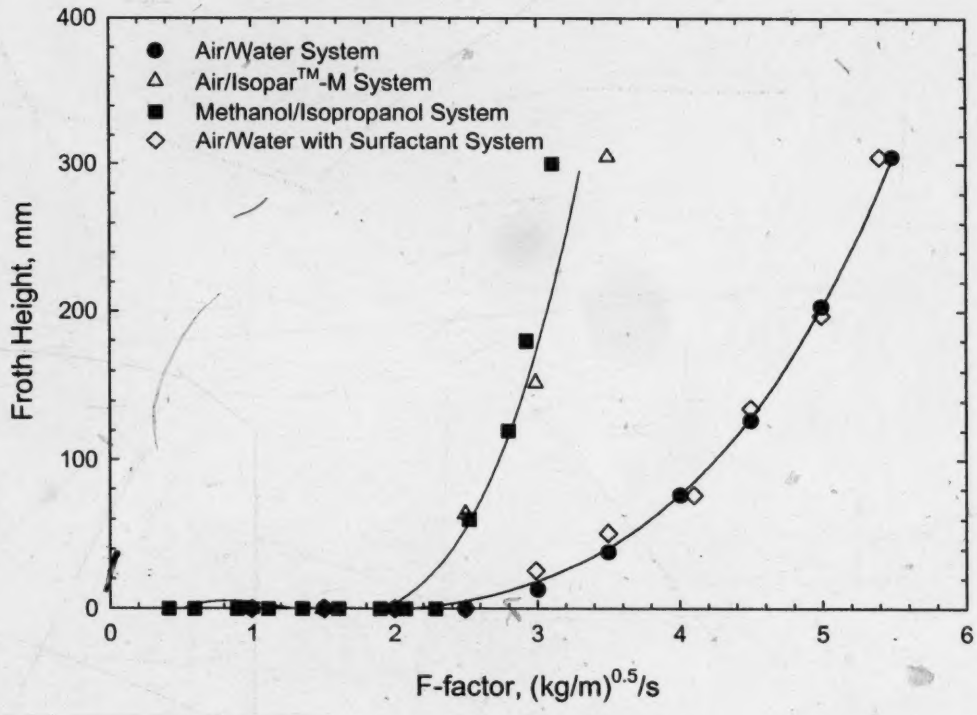

Figure 3.18. Comparison of the effect of system properties on froth height for a 76.2 mm thick SP-tray

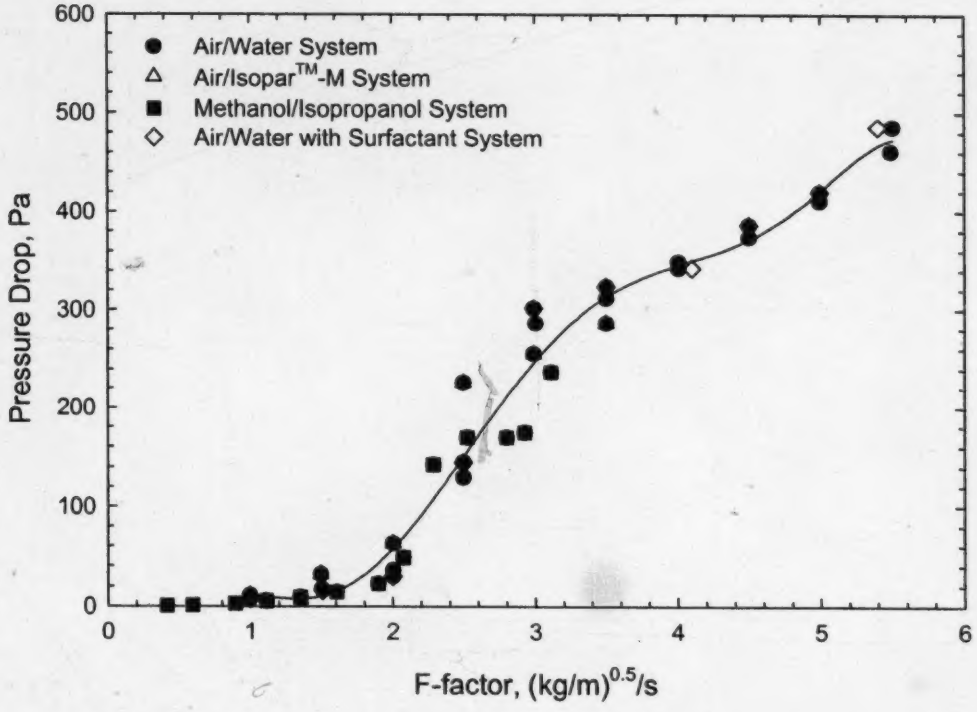

Figure 3.19. Comparison of the effect of system properties on total pressure drop for a 76.2 mm thick SP-tray

author's belief that the SP-tray could continuously out-perform the dualflow sieve tray as long as high density liquids or very high liquid rates are used in order to suppress this tendency for spray.

It is interesting to note the relative non-dependence of the physical properties on the froth height that can be seen in Figures 3.17 and 3.19. The pressure drop data for all four systems studied are very similar. This would indicate that the decrease in liquid density is offset by an increase in froth height to keep the total pressure drop constant for a given F-factor.

To help confirm the effect of the physical properties on the operation of a dualflow tray, several correlations were also employed to try and predict the performance of a dualflow tray. Since these correlations were developed for a dualflow sieve tray, experimental data for this type of tray were used for comparison. The correlations developed by Garcia and Fair (2002) and Ravagnani et al. (1990) were found to be inaccurate in predicting the froth height and were not included in this analysis. The correlations given by Xu et al. (1994) and Mahendru and Hackl (1979) did appear to predict the trend of the experimental data reasonably well. A comparison between the predictions of these two published correlations and experimentally obtained values for both air/water and methanol/isopropanol systems can be seen in Figure 3.20. Of these two correlations, the one given by Xu et al. (1994) best predicts the performance of the dualflow sieve tray both in air/water and methanol/isopropanol distillation systems.

$$h_f = \frac{h_L}{(1-\varepsilon)} \tag{3.2}$$

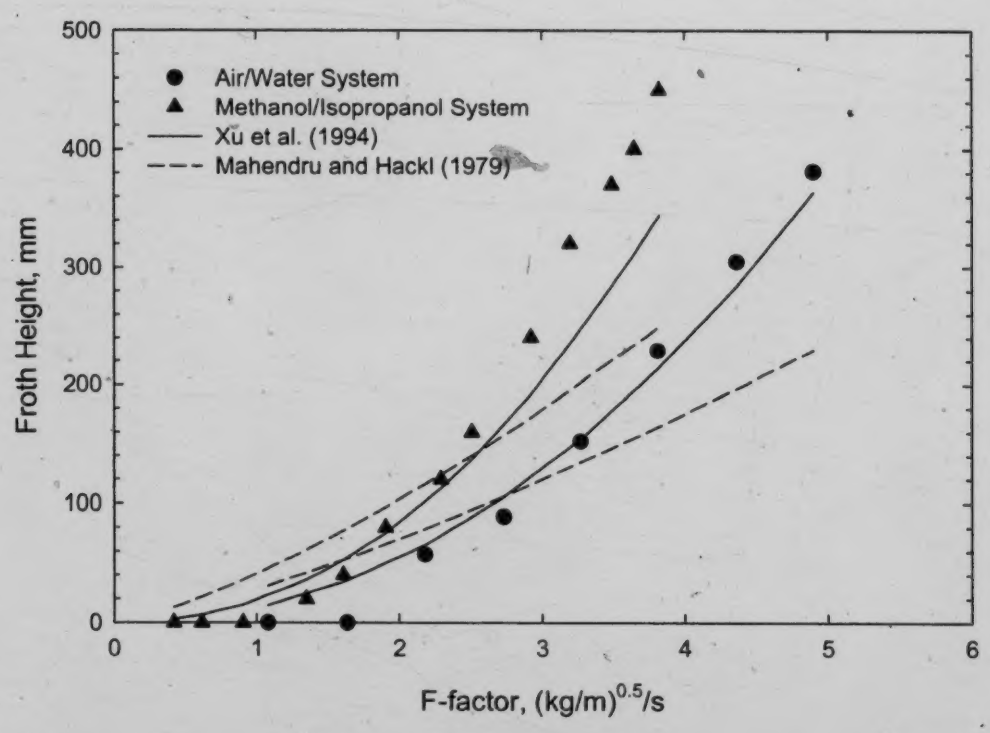

Figure 3.20. Comparison of measured and predicted froth heights using published correlations at L/V=1 for a dualflow sieve tray (36.1% open hole area)

where the porosity, ε, and clear liquid height, h_L, are given by

$$\varepsilon = 1.0 - 0.0946\left[\frac{U_s^2 \rho_G}{g h_L \rho_L}\right]^{-0.2} \tag{3.3}$$

$$h_L = 0.006\frac{(L M_L)^n \left(U_s (\rho_G / \rho_{air})^{0.5}\right)^{1.75}}{\rho_L \phi^{1.90} (T/d)^{0.42}} \tag{3.4}$$

and the parameter n is defined as a function of the tray open hole area, ϕ.

$$n = 0.3162\phi^{-0.25} \tag{3.5}$$

Since the correlation is only explicitly dependent on density effects and the vapour density effects are included in the F-factor already, it can be seen that the correlation accurately predicts the shift in capacity due to a change in liquid density. Although the constants in Equation (3.4) may include surface tension and viscosity effects, the manner in which the correlation is presented does not allow for an evaluation of these effects independently.

3.3. TRAY EFFICIENCY

Since, for the majority of the SP-tray's operation, no external froth existed on the surface of the tray, extracting liquid samples from the froth was not feasible. As well, when a froth existed, large concentration gradients (as high as 20%) across both the dualflow sieve and SP-trays were observed. As such, it was decided to take only two samples. Samples were taken from the bottom of the condenser (feed to the first tray) and the outlet of the fourth stage by means of a liquid collection trough system. Because the column was operated under total reflux, the Fenske (1932) equation could be used to calculate the number of theoretical stages, N_T, within the column.

$$N_T = \frac{\ln\left[\left(\frac{x_D}{1-x_D}\right)\left(\frac{1-x_B}{x_B}\right)\right]}{\ln \alpha_{avg}} \qquad (3.6)$$

where α_{avg} is the average relative volatility of the binary mixture. Because it is not constant for a methanol/isopropanol system, α_{avg} must be estimated as the geometric mean between the bottom, B, and distillate, D, compositions (Wankat, 1988).

$$\alpha_{avg} = \sqrt{\alpha_D \alpha_B} \qquad (3.7)$$

The relative volatility, α, can be calculated from equilibrium data provided by Wong (1993) using the liquid, x, and vapour, y, compositions.

$$\alpha = \frac{\frac{y}{x}}{\left(\frac{1-y}{1-x}\right)} \qquad (3.8)$$

The overall column efficiency, E_O, may now be calculated as,

$$E_O = \frac{N_T}{N_A} \qquad (3.9)$$

where N_A is the number of actual stages in the column. The overall column efficiency can then be converted to the Murphree tray efficiency, E_{MV}, using Equation (3.10).

$$E_{MV} = \frac{\lambda^{E_O} - 1}{\lambda - 1} \qquad (3.10)$$

where λ is known as the stripping factor and is defined as the ratio of the slope of the equilibrium line to the operating line and is given by

$$\lambda = \frac{mV}{L} \qquad (3.11)$$

where m is the slope of the equilibrium line. However, Equation (3.10) was developed based on the assumption that the equilibrium and operating lines are straight. Since constant molal overflow (CMO) is assumed and the column is operated under total reflux, the operating lines are straight and collapse onto the x=y line. As such, V/L=1 and λ=m. Because the slope of the equilibrium line changes with respective liquid concentrations, the arithmetic mean was used to find the slope between the distillate and bottoms compositions. To justify making such an assumption, an analysis was performed on the effect of the slope of the equilibrium line on the Murphree tray efficiencies obtained. Data were chosen at the highest efficiency for the 76.2 mm thick SP-tray which would represent the largest spread between the distillate and bottoms compositions. At this point, the Fenske equation provides approximately two theoretical stages. Taking the arithmetic means between distillate and bottoms compositions compared to the liquid composition between the two theoretical stages resulted in two separate values for each stage. The slope of the equilibrium line was then found at these points and used to calculate the Murphree efficiency based on those numbers. An average error of ±2.5% was found between the Murphree efficiency calculated using a column wide arithmetic mean and the theoretical stage arithmetic mean. Therefore, using the column wide arithmetic mean is justified.

Figure 3.21 shows the Murphree tray efficiencies for both the 76.2 and 114.3 mm thick SP-trays and the dualflow sieve tray as a function of vapour loading in distillation conditions. The Murphree tray efficiencies presented are a result of calculations using Equations (3.6) to (3.11). A plot of the overall column efficiency can be found in Appendix B. As stated previously (Section 3.2.1), two operating

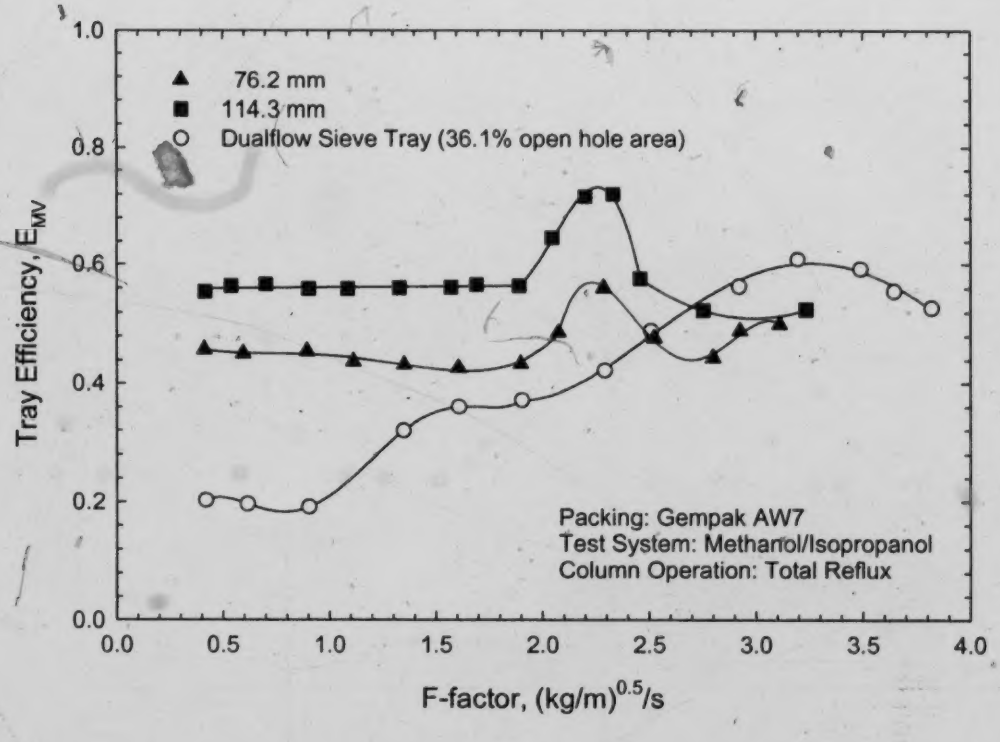

Figure 3.21. Comparison of Murphree tray efficiency between varying thickness of packing

zones exist for a dualflow sieve tray. From the figure, the first zone can be seen up to an F-factor of 1.3 $(kg/m)^{0.5}/s$. At an F-factor greater than this, the second operating zone, the data reflects the characteristic parabolic efficiency profile for a dualflow tray.

This figure also shows a unique efficiency profile for the SP-tray. The trend in efficiency also corresponds to the four operating zones described previously (Section 3.2.1). In the free-flow zone (F-factor up to 1.9 $(kg/m)^{0.5}/s$), the efficiency remains fairly constant since there is no change in the liquid holdup within the tray itself. The loading zone (F-factor from 1.9 to 2.3 $(kg/m)^{0.5}/s$) is characterized by a sharp increase in efficiency until a peak efficiency is reached. This peak represents the dynamic liquid flood point. In the blow-out zone (F-factor from 2.3 to 2.8 $(kg/m)^{0.5}/s$) the efficiency decreases rapidly as the froth moves out of the tray onto the packing surface. This indicates that the dynamic froth within the tray is much more efficient in promoting mass transfer compared to a surface froth which, as stated earlier, appears to be a spray. The final froth-dominated zone (F-factor greater than 2.8 $(kg/m)^{0.5}/s$) is seen as a slight increase in efficiency once again due to a buildup in froth height. Notice how the efficiency curves for both the 76.2 and 114.3 mm thick SP-trays appear to converge. This indicates that the tray itself no longer has any significant contribution to mass transfer and that the mass transfer is only governed by the froth on the surface of the tray. Since is was seen from Figure 3.11 that the froth heights were nearly identical for both SP-trays at a given F-factor, it is logical to expect the same efficiencies given the same froth height.

From Figure 3.21, it is important to note the difference in efficiency between the dualflow sieve tray and the SP-tray at very low vapour loadings; where no froth exists on the surface of the tray. An efficiency increase of 130% is observed between the 76.2 mm thick SP-tray and the dualflow sieve tray at an F-factor of 0.5 $(kg/m)^{0.5}/s$. This increase in efficiency is a result of the increased vapour-liquid contact time present in the SP-tray due to the liquid film flowing down through the tray.

Additional experiments were carried out to determine the amount of mass transfer occurring without the presence of any trays in the column; when the column is operated as a spray tower. A maximum liquid concentration difference of 5% was observed between the liquid at the top and bottom of the tower. Because these differences were minimal, they were included in the overall column efficiency calculations.

At lower vapour loadings, the efficiency of the SP-tray is superior to the dualflow sieve tray. However, at very high vapour loadings, the efficiency drops off substantially due to severe entrainment causing the dualflow sieve tray to be more suitable for high capacity operations. However, at any F-factor of approximately 2.5 (where the efficiency curves between the SP-trays and the dualflow sieve trays cross) or lower in a methanol/isopropanol system, it is clear that the choice of tray would be the SP-tray.

3.4. HETP

Since the SP-tray is essentially a thin slice of structured packing, an analysis was performed to compare the SP-tray to a fully packed column. To do this, the

height equivalent to a theoretical plate (HETP) method was used. A comparison of the HETP for the SP-tray and a fully packed column can be found in Figure 3.22. The overall heights of a transfer unit, H_{OG}, for a fully packed column were provided by Xu et al. (2000) and converted to HETP values using the following equation.

$$HETP = H_{OG} \frac{\ln\lambda}{\lambda - 1} \tag{3.12}$$

In order to obtain a value of the slope of the equilibrium line needed to find the HETP values through the stripping factor, the arithmetic mean was found between the limits of liquid composition presented in the paper.

The values of HETP for the SP-tray were calculated using the number of theoretical stages found from the Fenske equation.

$$HETP = \frac{z}{N_T} \tag{3.13}$$

The value of the packing thickness, z, was determined by summing up the total amount of packing in the tower. For the case of the 76.2 mm thick SP-tray, four trays were used which gives a total packing depth of 304.8 mm; the distance between the trays is neglected.

As expected, the HETP trend for the SP-tray is essentially the inverted trend of the Murphree tray efficiency. However, a very interesting concern can now be raised. Since all three curves represent the same packing, they should all lie on the same line. The HETP curve should be constant for a given type of packing. But, as can be seen, three distinct curves exist. This indicates that additional phenomena are occurring when the packing is used as an SP-tray that do not exist in a fully packed column. The reason for this separation in HETP curves could be explained by the continual

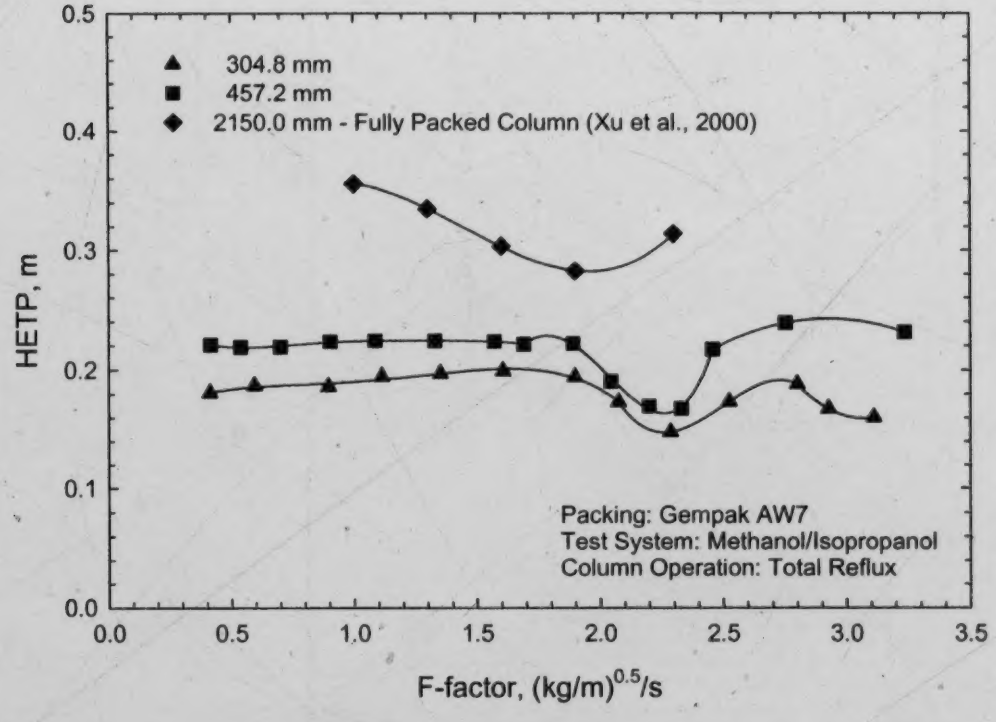

Figure 3.22. Comparison of HETP values between varying thickness of packing

redistribution of liquid in the space between each tray. Since it is known that liquid maldistribution occurs in structured packings with the liquid migrating toward the column walls, this continual redistribution of liquid could significantly affect the overall column efficiency. As well, as stated by Garcia and Fair (2002), 0.1-0.2 theoretical stages can exist in the spray zone above the froth on a dualflow tray. Both of these two factors are believed to be the cause in the 30 to 50% decreases in HETP values compared to a fully packed column. This may indicate that having a fully packed column is not necessarily the best design for distillation applications. A column may only need to have small sections of packing, say 76.2-101.6 mm, with small void spaces between each section. Having such a column could dramatically increase the overall column efficiency and significantly reduce the total pressure drop. However, to confirm such a hypothesis further testing is required.

3.5. TRAY MIXING

A qualitative analysis was performed on the extent of mixing present on both the 76.2 mm thick SP-tray and a dualflow sieve tray. An aqueous solution of crystal violet was injected at both the centre and outer edge of each tray.

Through visual observation, the level of mixing on the SP-tray appeared to be higher than that of the dualflow sieve tray. Concentrated pockets of colour remained on the dualflow sieve tray while the SP-tray had a much more uniform colour distribution within the froth layer. This observation would indicate that there exists a higher degree of mixing on the SP-tray versus the dualflow sieve tray.

Through the use of dye, the concept of segmented regions of liquid dumping and the formation of hydrodynamic waves presented in open literature was verified. On the dualflow sieve tray, the crest of such a wave is evidenced by an increase in the intenseness of the crystal violet colour due to an increased liquid depth. From below the tray looking up through the sieve holes, the waves can be seen as dark patches of colour moving around the tray deck. Dark patches of colour indicate where the segmented zones of liquid dumping occur. This dumping is the result of the greater hydrodynamic head present at a crest versus a trough.

Since liquid bypassing through zones of liquid dumping decreases the overall residence time of the liquid on the tray, this will generally have a negative effect on the tray's efficiency. Therefore, it is believed that the visually observed increase in liquid mixing on the SP-tray compared to a dualflow sieve tray may help suppress the effect of liquid bypassing by promoting mixing on the tray deck. This, in turn, would help to eliminate concentration gradients, thus increasing tray efficiency.

Chapter 4

CONCLUSIONS AND RECOMENDATIONS

This thesis presents an in-depth study of a novel design for a new type of dualflow distillation tray; the SP-tray. Emphasis was placed on examining the hydraulic and efficiency performance as compared to a commercially available dualflow sieve tray.

Initial hydraulic studies in an air/water system revealed that the SP-tray had an increased capacity while no appreciable benefit in pressure drop reduction was noted. However, in distillation conditions using a methanol/isopropanol system, a decrease in capacity was observed. This decrease was determined to be a result of the SP-tray's affinity for operating in the spray regime which causes an increased proneness to entrainment especially at lower liquid densities. The dependence of the stable operating range on the liquid density for an SP-tray was found to be significantly higher than that for a dualflow sieve tray.

Mass transfer studies conducted in a distillation column revealed that the SP-tray has a relatively high efficiency compared to the dualflow sieve tray, especially at low vapour velocities. This demonstrates that the SP-tray has a higher turndown compared to the dualflow sieve tray in terms of mass transfer. However, due to the SP-tray's increased susceptibility to liquid entrainment at high vapour loadings, especially in lower density liquids, capacity limits seen were less than those for the dualflow sieve tray. It is recommended that further testing of the SP-tray be conducted in distillation and absorption conditions using higher density liquids. It is

believed that these conditions will show not only an increase in efficiency at lower vapour loadings but also at higher vapour loadings as a result of the increased capacity observed with higher density liquids.

Interesting results were found when the SP-tray was compared to a fully packed column using the HETP method. Significant reductions in HETP were observed when the packing was used as a tray with an appreciable spacing between each tray. It is speculated that this is a result of a continual redistribution of the liquid throughout the column and an appreciable amount of mass transfer occurring in the spray zone between the trays. As such, it is recommended that further testing of this phenomenon be conducted by placing small sections of packing in a column with spacing between them. This testing may indicate that completely filling a column with packing is unnecessary and that significant pressure loss savings can be recovered.

Overall, it is the author's belief that the SP-tray is a higher capacity, higher efficiency tray than the dualflow sieve tray given the right operating conditions. With the observed increased efficiencies and turndown ratios, further studies into the use of the SP-tray commercially are justified.

Chapter 5

REFERENCES

Baird, J.L. Letter to the Editor. Chem. Eng. Prog. **95**(5), 7 (1999).

Billet, R., "A Contribution to the Evaluation of Mass Transfer Trays", Chem. Eng. Tech. **20**(4), 221-229 (1997).

Billet, R., "Distillation Engineering", Chemical Publishing Co., Inc., New York (1979).

Billet, R., "Separation Tray without Downcomers", Chem. Eng. Tech. **24**(11), 1103-1112 (2001).

Billet, R., S. Conrad and C.M. Grubb, "Some Aspects of the Choice of Distillation Equipment", Inst. Chem. Eng. Symp. Ser. No. 32 5/111-126 (1969).

Furzer, I.A., "Froth Heights on Dual-Flow Trays with a Heterogeneous Binary Azeotropic System and a Heterogeneous Ternary System with a Homogeneous Azeotrope", Ind. Eng. Chem. Res. **40**(22), 4951-4966 (2001).

Furzer, I.A., "Froth Heights on Dualflow Trays with a Ternary Azeotropic System of Ethyl Acetate-Ethanol-Water", Ind. Eng. Chem. Res. **39**(5), 1430-1436 (2000).

Garcia, J.A., and J.R. Fair, "Distillation Sieve Trays without Downcomers: Prediction of Performance Characteristics", Ind. Eng. Chem. Res. **41**(6), 1632-1640 (2002).

Garner, F.H., S.R.M. Ellis and D.C. Freshwater, "The Comparison of Vapor-Liquid Contacting Apparatus", Trans. Inst. Chem. Eng. **35**, 61-68 (1957).

Hutchinson, M.H. and R.F. Baddour, "Ripple Trays – A New Tool for Vapor-Liquid Contacting", Chem. Eng. Prog. **52**(12), 503-508 (1956).

Kister, H.Z., "Distillation Design", McGraw-Hill, Inc., New York (1992).

Kreis, H. and M. Raab, "Industrial Application of Sieve Trays with Hole Diameters from 1 to 25 mm with and without Downcomers", Inst. Chem. Eng. Symp. Ser. No. 56 3.2/63-83 (1979).

Mahendru, H.L. and A. Hackl, "Contribution to the Design of Sieve Trays without Downcomers", Inst. Chem. Eng. Symp. Ser. No. 56, 3.2/35-46 (1979).

Miyahara, T. and T. Takahashi, "Sizes of Droplets Produced in the Jetting Regime at Single Orifices", J. Chem. Eng. Jap. **17**(2), 218-220 (1984).

Miyahara, T., H. Terakado and T. Takahashi, "Transition from Bubbling to Jetting at Single Orifices", J. Chem. Eng. Jap. **16**(6), 454-458 (1983).

Miyahara, T., M. Kurihara, M. Asoda and T. Takahashi, "Gas-Liquid Interfacial Area and Liquid-Phase Mass Transfer Coefficient in Sieve Plate Columns without Downcomer Operating at High Gas Velocities", J. Chem. Eng. Japan **23**(3), 280-285 (1990).

Molokanov, Y.K., A.I. Sloblo, S.A. Kruglov and V.A. Shchelkunov, "New Designs for Contact Devices in Distillation Towers", Chem. Tech. Fuels and Oils **16**(7), 450-456 (1980).

Payne, G.J. and R.G.H. Prince, "The Relationship Between the Froth and Spray Regimes, and the Orifice Processes Occurring on Perforated Distillation Plates", Trans. Inst. Chem. Eng. **55**, 266-273 (1977).

Payne, G.J. and R.G.H. Prince, "The Transition from Jetting to Bubbling at a Submerged Orifice", Trans. Inst. Chem. Eng. **53**, 209-223 (1975).

Pfeiffenberger, C.A., "Tower Utilizes Kinetic Energy", Chem. Eng. **60**(4), 242-243 (1953).

Pollard, B., "The Kittel Plate", Trans. Inst. Chem. Eng. **35**, 69-75 (1957).

Ravagnani, T.M.K., J.A.F.R. Pereira and P.A.S. Gunther, "The Hydrodynamic Behaviour of Sieve Trays without Downcomers", Proc. Can. Chem. Eng. Conf., Halifax, NS, July, 14-21 (1990).

Rylek, M. and G. Standart, "The Hydraulics of Sieve Trays", Int. Chem. Eng. **4**(4), 711-747 (1964).

Sharma, M.M. and R.K. Gupta, "Mass Transfer Characteristics of Plate Columns without Downcomer", Trans. Inst. Chem. Eng. **45**, T169-T175 (1967).

Shell Development Company, "Turbogrid Distillation Trays", Chem. Eng. Prog. 50(2), 57-64 (1954).

Shoukry, E., J. Cermak and V. Kolar, "On the Hydrodynamics of Sieve Plates Without Downcomers. 1. Dynamic Nature of Gas-Liquid Dispersions", Chem. Eng. J. **8**, 27-40 (1974).

Shoukry, E. and V. Kolar, "On the Hydrodynamics of Sieve Plates Without Downcomers. 2. A Model of Plate Operation and the Phenomena of Multiplicity of State", Chem. Eng. J. **8**, 41-51 (1974).

Sloley, A.W., "Should You Switch to High Capacity Trays?", Chem. Eng. Prog. **95**(1), 23-35 (1999).

Solomakha, G.P. and A.N. Planovskii, "The Relationship Between Mass Transfer in the Gas Phase and Bubble Hydraulic Parameters (Bubble Cap and Drip Plates)", Int. Chem. Eng. **3**(2), 264-268 (1963).

Steiner L. and G. Standart, "Studies on Distillation XV. Liquid Holdup on Plates without Downcomers", Coll. Czech. Chem. Comm. **32**, 89-100 (1967).

Steiner L. and G. Standart, "Studies on Distillation XVI. Pressure Drop Across Plates without Downcomers", Coll. Czech. Chem. Comm. **32**, 101-115 (1967).

Takahashi, T., Y. Akagi and T. Kishimoto, "Gas and Liquid Velocities at Incipient Liquid Stagnation of a Sieve Tray", Int. Chem. Eng. **19**(1), 113-118 (1979).

Takahashi, T., T. Miyahara and K. Shimizu, "Experimental Studies of Gas Void Fractions and Froth Height on a Perforated Plate", J. Chem. Eng. Jap. **7**(2), 75-80 (1974).

Takahashi, T., T. Miyahara, T. Tano and Y Akagi, "Hydrodynamic Characteristics of Sieve Trays Having Large Free Areas without Downcomers", J. Chem. Eng. Japan **19**(4), 339-341 (1986).

Van den Berg, G.J., "Commercial Application of Turbogrid Trays", Trans. Inst. Chem. Eng. **35**, 409-412 (1957).

Wankat, P.C., "Equilibrium Staged Separations", Prentice Hall, New Jersey (1988).

Weiland, R.H., "Hydraulic Stability of Dualflow Trays", for AIChE Spring National Meeting, April 25, Houston, Texas (2001).

Wong, A.K.M., "New Correlations for Predicting Sieve Tray Efficiencies", M.Sc. Thesis (1993).

Xu, Z.P., A. Afacan and K.T. Chuang, "Efficiency of Dualflow Trays in Distillation", Can. J. Chem. Eng. **72**(4), 607-613 (1994).

Young, D.F., B.R. Munson and T.H. Okiishi, "A Brief Introduction to Fluid Mechanics", John Wiley & Sons Inc., Toronto (1997).

Appendix A

EXPERIMENTAL DATA

Table A.1. Experimental dry tray pressure drop data

38.1 mm		76.2 mm		114.3 mm	
F-factor ($(kg/m)^{0.5}/s$)	Pressure Drop (Pa)	F-factor ($(kg/m)^{0.5}/s$)	Pressure Drop (Pa)	F-factor ($(kg/m)^{0.5}/s$)	Pressure Drop (Pa)
0.74	2.5	0.75	3.0	0.76	4.7
1.48	7.5	1.50	10.2	1.48	14.9
2.23	14.4	2.23	21.2	2.23	30.9
2.97	24.2	2.97	35.6	2.97	51.8
3.71	35.9	3.71	54.1	3.71	77.7
4.45	49.8	4.45	74.5	4.45	109.1
5.19	66.0	5.19	98.1	5.19	142.2

254.0 mm		Dualflow Sieve Tray	
F-factor ($(kg/m)^{0.5}/s$)	Pressure Drop (Pa)	F-factor ($(kg/m)^{0.5}/s$)	Pressure Drop (Pa)
0.74	10.0	0.80	2.5
1.48	30.6	1.62	9.5
2.23	62.3	2.42	20.2
2.97	102.6	3.23	36.9
3.71	153.7	4.04	57.8
4.45	212.2	4.85	83.4
5.19	279.0	5.65	112.6

Table A.2. Experimental dynamic liquid holdup data

Liquid Rate = 12.5 $m^3/h \cdot m^2$			
76.2 mm		114.3 mm	
F-factor $((kg/m)^{0.5}/s)$	Pressure Drop (Pa)	F-factor $((kg/m)^{0.5}/s)$	Pressure Drop (Pa)
0.74	5.5	0.74	8.0
1.50	18.7	1.50	27.9
1.87	31.1	2.26	120.3
2.23	93.8	2.50	143.5
2.47	117.1	2.72	178.7
2.72	149.4	2.97	250.3
2.97	205.5	3.09	292.7
3.07	262.8	3.16	358.7
		3.21	382.3

Liquid Rate = 24.9 $m^3/h \cdot m^2$					
38.1 mm		76.2 mm		114.3 mm	
F-factor $((kg/m)^{0.5}/s)$	Pressure Drop (Pa)	F-factor $((kg/m)^{0.5}/s)$	Pressure Drop (Pa)	F-factor $((kg/m)^{0.5}/s)$	Pressure Drop (Pa)
0.73	5.2	0.74	8.2	0.77	11.5
0.99	8.2	1.12	15.9	1.50	44.8
1.24	11.7	1.50	29.3	1.73	78.7
1.48	16.2	1.73	55.7	1.99	114.0
1.73	24.7	1.98	93.4	2.25	154.2
1.98	94.7	2.23	127.0	2.35	192.4
2.23	129.5	2.35	241.6	2.47	288.9
2.32	154.4			2.57	373.6

254.0 mm	
F-factor $((kg/m)^{0.5}/s)$	Pressure Drop (Pa)
0.74	18.7
0.99	30.1
1.24	45.6
1.48	64.8
1.73	127.0
1.98	183.1
2.23	523.1
2.29	822.0

Liquid Rate = 37.3 $m^3/h \cdot m^2$					
38.1 mm		76.2 mm		114.3 mm	
F-factor $((kg/m)^{0.5}/s)$	Pressure Drop (Pa)	F-factor $((kg/m)^{0.5}/s)$	Pressure Drop (Pa)	F-factor $((kg/m)^{0.5}/s)$	Pressure Drop (Pa)
0.73	6.0	0.74	9.0	0.73	12.2
0.99	9.5	1.00	14.4	1.51	61.9
1.24	14.4	1.25	20.4	1.73	94.7
1.50	20.7	1.48	31.8	1.98	131.4
1.73	84.7	1.73	76.0	2.11	168.1
1.98	121.4	1.97	107.7	2.25	302.6
2.15	158.2	2.10	236.6	2.27	383.6

Liquid Rate = 49.7 $m^3/h \cdot m^2$					
38.1 mm		76.2 mm		254.0 mm	
F-factor $((kg/m)^{0.5}/s)$	Pressure Drop (Pa)	F-factor $((kg/m)^{0.5}/s)$	Pressure Drop (Pa)	F-factor $((kg/m)^{0.5}/s)$	Pressure Drop (Pa)
0.74	8.0	0.74	10.0	0.73	22.4
0.99	12.2	0.99	16.2	0.99	39.9
1.25	18.6	1.25	28.0	1.24	58.9
1.48	26.8	1.48	49.6	1.48	105.2
1.73	99.6	1.73	88.8	1.73	204.9
1.98	140.7	1.95	234.1	1.84	772.2
2.01	155.7				

Table A.3. Experimental data on hydraulic performance in air/water column

Liquid Rate = 12.5 $m^3/h \cdot m^2$					
76.2 mm			114.3 mm		
F-factor $((kg/m)^{0.5}/s)$	Froth Height (mm)	Pressure Drop (Pa)	F-factor $((kg/m)^{0.5}/s)$	Froth Height (mm)	Pressure Drop (Pa)
3.58	25	292.7	3.34	38	444.6
3.93	44	313.8	3.66	51	458.3
4.25	64	322.6	4.01	76	477.0
4.62	76	336.3	4.33	102	503.1
4.94	89	343.7	4.67	127	523.1
5.32	102	361.2	5.02	165	541.8
5.64	127	382.3	5.34	229	570.4
			5.66	330	591.6

Liquid Rate = 24.9 $m^3/h \cdot m^2$					
38.1 mm			76.2 mm		
F-factor $((kg/m)^{0.5}/s)$	Froth Height (mm)	Pressure Drop (Pa)	F-factor $((kg/m)^{0.5}/s)$	Froth Height (mm)	Pressure Drop (Pa)
3.41	38	217.9	2.40	25	306.4
3.73	64	236.6	2.72	38	323.8
4.10	89	255.3	3.07	51	330.0
4.43	114	269.0	3.39	64	342.5
4.75	140	282.7	3.71	76	367.4
5.12	165	298.9	4.10	89	378.6
5.44	191	320.1	4.45	102	392.3
			4.75	127	414.7
			5.09	178	435.9
			5.44	305	485.7

114.3 mm			Dualflow Sieve Tray		
F-factor $((kg/m)^{0.5}/s)$	Froth Height (mm)	Pressure Drop (Pa)	F-factor $((kg/m)^{0.5}/s)$	Froth Height (mm)	Pressure Drop (Pa)
2.15	38	439.6	1.25	25	111.1
2.50	76	510.6	1.63	51	134.1
2.82	114	553.0	1.99	76	158.2
3.16	127	557.9	2.36	102	200.5
3.46	152	572.9	2.72	152	242.9
3.81	203	617.7	3.10	178	269.0
4.13	254	660.1	3.45	203	287.7
4.47	330	709.9	3.77	229	313.8
			4.15	279	342.5
			4.50	330	373.6
			4.85	406	392.3

Liquid Rate = 37.3 $m^3/h \cdot m^2$					
38.1 mm			76.2 mm		
F-factor $((kg/m)^{0.5}/s)$	Froth Height (mm)	Pressure Drop (Pa)	F-factor $((kg/m)^{0.5}/s)$	Froth Height (mm)	Pressure Drop (Pa)
3.39	38	237.9	2.03	38	327.5
3.76	64	270.3	2.37	51	353.7
4.08	89	286.4	2.72	70	357.4
4.43	127	306.4	3.07	76	366.2
4.75	178	323.8	3.41	89	383.6
5.12	229	342.5	3.76	114	414.7
5.41	279	373.6	4.08	152	477.0
5.71	356	423.4	4.40	203	510.6
			4.75	254	541.8
			5.09	330	560.4

114.3 mm		
F-factor $((kg/m)^{0.5}/s)$	Froth Height (mm)	Pressure Drop (Pa)
1.84	38	445.9
2.18	89	555.5
2.50	114	585.3
2.84	140	597.8
3.19	178	616.5
3.49	229	666.3
3.86	305	734.8

Liquid Rate = 49.7 $m^3/h \cdot m^2$					
38.1 mm			76.2 mm		
F-factor $((kg/m)^{0.5}/s)$	Froth Height (mm)	Pressure Drop (Pa)	F-factor $((kg/m)^{0.5}/s)$	Froth Height (mm)	Pressure Drop (Pa)
3.07	38	213.0	1.85	38	336.3
3.41	51	260.3	2.20	64	373.6
3.73	76	286.4	2.55	76	386.1
4.08	127	311.4	2.89	89	398.5
4.40	178	336.3	3.21	114	419.7
4.75	229	342.5	3.54	152	467.0
5.07	279	367.4	3.91	203	523.1
5.44	330	435.9	4.23	254	566.7
5.74	381	485.7	4.57	330	597.8

114.3 mm			Dualflow Sieve Tray		
F-factor $((kg/m)^{0.5}/s)$	Froth Height (mm)	Pressure Drop (Pa)	F-factor $((kg/m)^{0.5}/s)$	Froth Height (mm)	Pressure Drop (Pa)
1.69	51	473.3	0.94	25	109.6
2.03	102	591.6	1.31	51	150.7
2.40	140	610.3	1.67	76	186.8
2.69	178	632.7	2.05	102	259.0
3.04	229	685.0	2.41	152	291.4
3.34	279	759.7	2.77	178	340.0
3.68	330	822.0	3.12	229	379.9
			3.45	279	417.2
			3.77	330	435.9
			4.15	406	460.8

Table A.4. Experimental data on distillation performance

76.2 mm				
F-factor ($(kg/m)^{0.5}/s$)	Froth Height (mm)	Pressure Drop (Pa)	Tray 1-in (area % MeOH)	Tray 4-out (area % MeOH)
0.41	0	0.5	71.840	43.100
0.59	0	1.0	75.042	47.638
0.89	0	2.7	76.067	48.774
1.11	0	5.2	76.137	50.100
1.35	0	9.0	75.865	50.095
1.61	0	14.2	74.925	49.217
1.90	0	22.4	73.806	47.245
2.07	0	48.6	77.441	48.428
2.29	0	142.0	79.612	46.140
2.52	60	169.4	72.900	43.036
2.80	120	169.4	72.870	45.292
2.93	180	174.4	71.374	40.379
3.11	300	236.6	67.350	35.226

114.3 mm				
F-factor ($(kg/m)^{0.5}/s$)	Froth Height (mm)	Pressure Drop (Pa)	Tray 1-in (area % MeOH)	Tray 4-out (area % MeOH)
0.42	0	1.2	74.611	39.867
0.54	0	3.0	77.488	42.906
0.70	0	4.0	79.192	45.103
0.90	0	5.7	80.018	46.879
1.09	0	10.0	80.711	47.941
1.33	0	14.9	81.265	48.715
1.57	0	20.7	81.305	48.685
1.69	0	25.7	81.012	47.897
1.89	0	34.9	80.751	47.620
2.05	0	64.8	83.404	45.794
2.20	0	112.1	85.844	44.730
2.33	0	194.3	83.785	40.985
2.46	0	194.3	81.393	47.759
2.75	40	204.2	77.564	45.910
3.23	300	423.4	70.608	37.154

Dualflow Sieve Tray				
F-factor ((kg/m)$^{0.5}$/s)	Froth Height (mm)	Pressure Drop (Pa)	Tray 1-in (area % MeOH)	Tray 4-out (area % MeOH)
0.42	0	1.2	60.008	47.093
0.62	0	2.0	63.295	51.056
0.90	0	3.7	63.499	51.615
1.35	20	48.6	69.557	49.922
1.61	40	64.8	70.891	48.736
1.90	80	79.7	71.154	48.271
2.29	120	94.7	73.811	48.045
2.51	160	114.6	76.746	47.189
2.92	240	144.5	78.744	44.690
3.20	320	164.4	78.023	40.487
3.49	370	211.7	74.962	37.693
3.65	400	261.5	72.618	37.427
3.82	450	298.9	70.438	36.770

Table A.5. Experimental data at L/V=1 in air/water column

76.2 mm			
F-factor ($(kg/m)^{0.5}/s$)	Liquid Rate (kg/s)	Froth Height (mm)	Pressure Drop (Pa)
0.99	0.08	0	8.7
1.50	0.12	0	17.4
2.00	0.15	0	36.1
2.50	0.19	0	129.5
3.00	0.23	13	286.4
3.50	0.27	38	311.4
4.01	0.31	76	348.7
4.50	0.35	127	373.6
4.99	0.38	203	411.0
5.49	0.42	305	460.8

Dualflow Sieve Tray			
F-factor ($(kg/m)^{0.5}/s$)	Liquid Rate (kg/s)	Froth Height (mm)	Pressure Drop (Pa)
1.08	0.08	0	7.0
1.64	0.12	0	15.2
2.18	0.16	57	120.8
2.73	0.19	89	147.0
3.27	0.23	152	213.0
3.81	0.27	229	261.5
4.36	0.31	305	311.4
4.90	0.35	381	367.4

Table A.6. Experimental data at L/V=1 in air/water column with surfactant

76.2 mm			
F-factor ($(kg/m)^{0.5}/s$)	Liquid Rate (kg/s)	Froth Height (mm)	Pressure Drop (Pa)
1.00	0.08	0	7.5
1.51	0.12	0	15.7
2.00	0.15	0	29.9
2.50	0.19	0	144.5
2.99	0.23	25	301.4
3.50	0.27	51	323.8
4.01	0.31	76	342.5
4.50	0.35	127	386.1
4.99	0.38	203	419.7
5.50	0.43	305	485.7

Dualflow Sieve Tray			
F-factor ($(kg/m)^{0.5}/s$)	Liquid Rate (kg/s)	Froth Height (mm)	Pressure Drop (Pa)
1.09	0.08	0	6.5
1.64	0.12	0	13.7
2.18	0.15	51	122.1
2.72	0.19	95	149.4
3.26	0.23	152	211.7
3.81	0.27	229	255.3
4.36	0.31	305	311.4
4.90	0.35	381	373.6

Table A.7. Experimental data at L/V=1 in air/Isopar™-M column

76.2 mm			
F-factor ($(kg/m)^{0.5}/s$)	Liquid Rate (kg/s)	Froth Height (mm)	Pressure Drop (Pa)
1.00	0.08	0	10.7
1.50	0.12	0	31.9
2.00	0.15	0	62.9
2.50	0.19	64	226.0
2.99	0.23	152	255.3
3.50	0.27	305	286.4

Dualflow Sieve Tray			
F-factor ($(kg/m)^{0.5}/s$)	Liquid Rate (kg/s)	Froth Height (mm)	Pressure Drop (Pa)
1.09	0.08	0	7.0
1.64	0.12	64	74.0
2.18	0.15	114	93.4
2.72	0.19	203	137.0
3.27	0.23	305	189.3
3.81	0.27	432	247.8

Appendix B

ADDITIONAL FIGURES

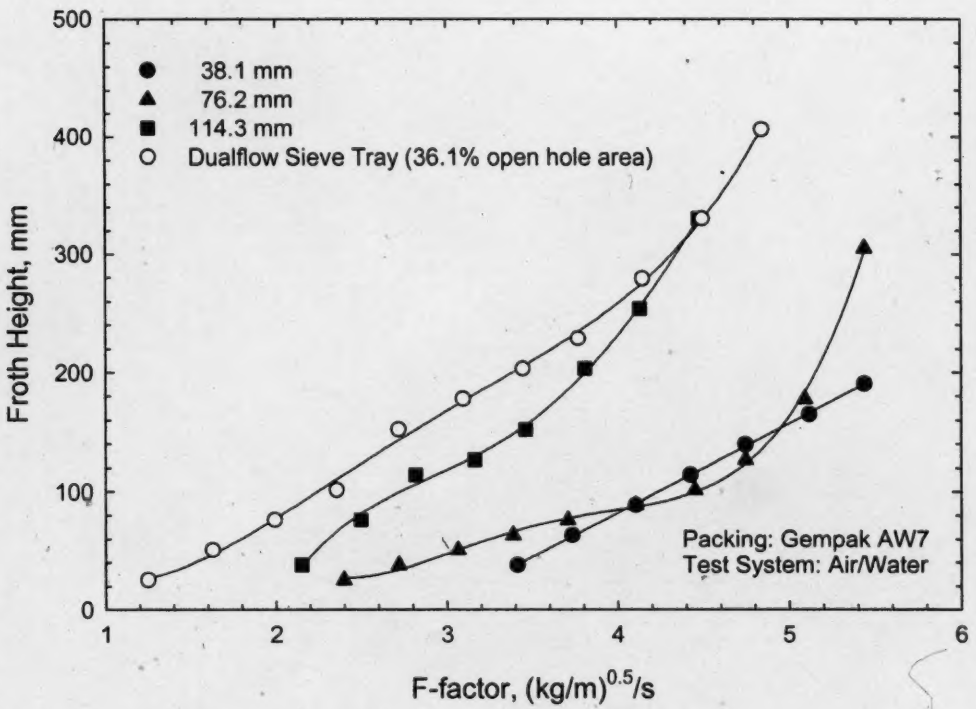

Figure B.1. Comparison of froth height between varying thickness of packing at a liquid flowrate of 24.9 $m^3/h \cdot m^2$

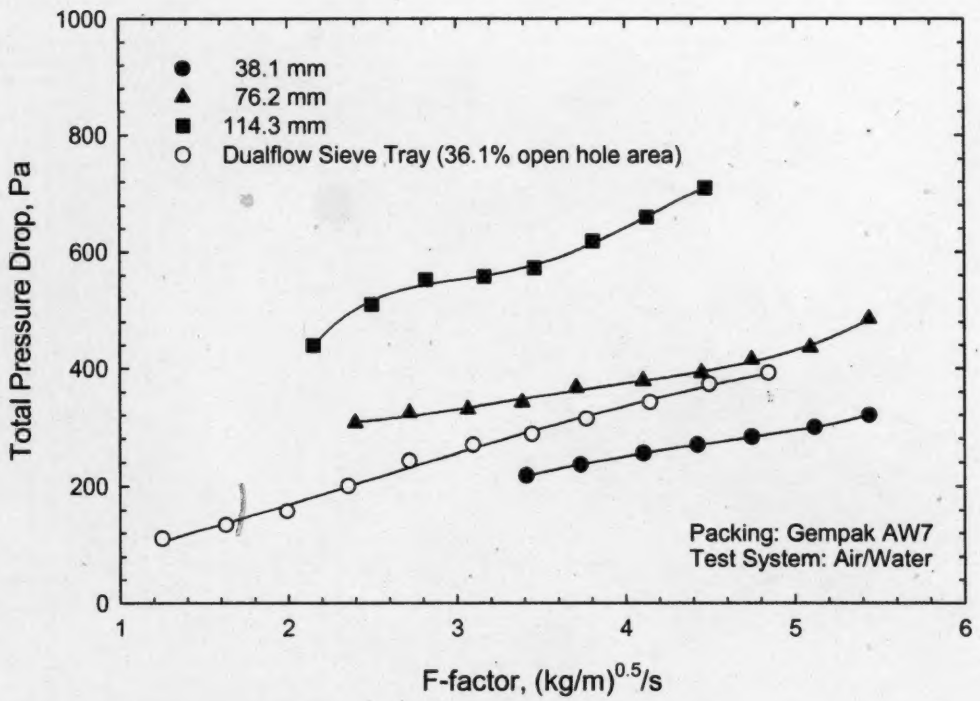

Figure B.2. Comparison of total pressure drop between varying thickness of packing at a liquid flowrate of 24.9 $m^3/h \cdot m^2$

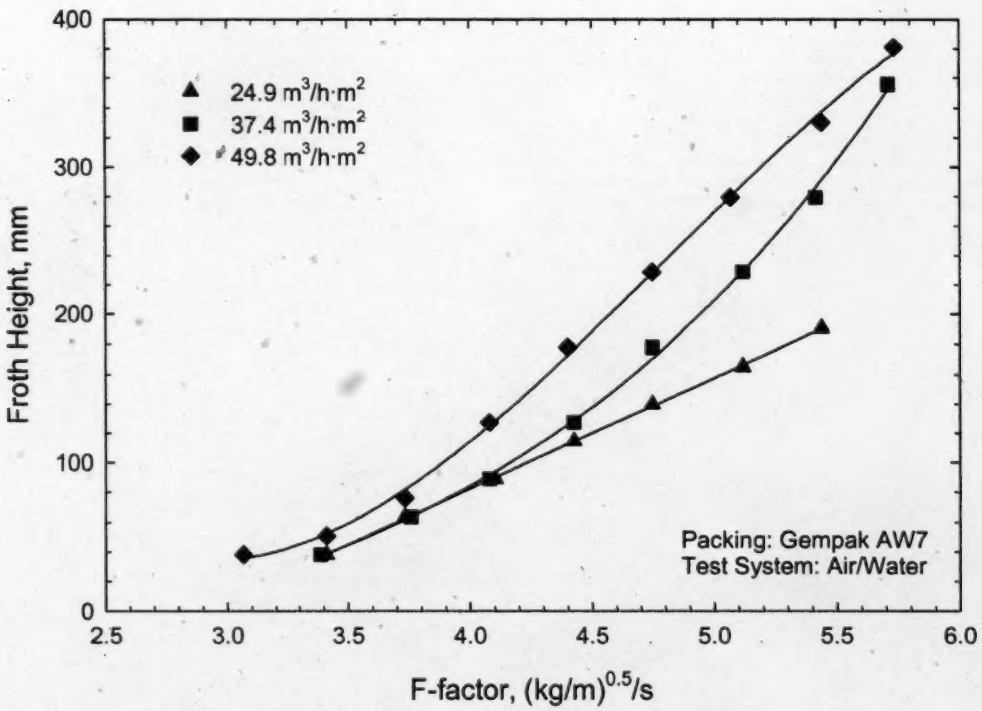

Figure B.3. Comparison of froth height between varying liquid flowrates at a packing thickness of 38.1 mm

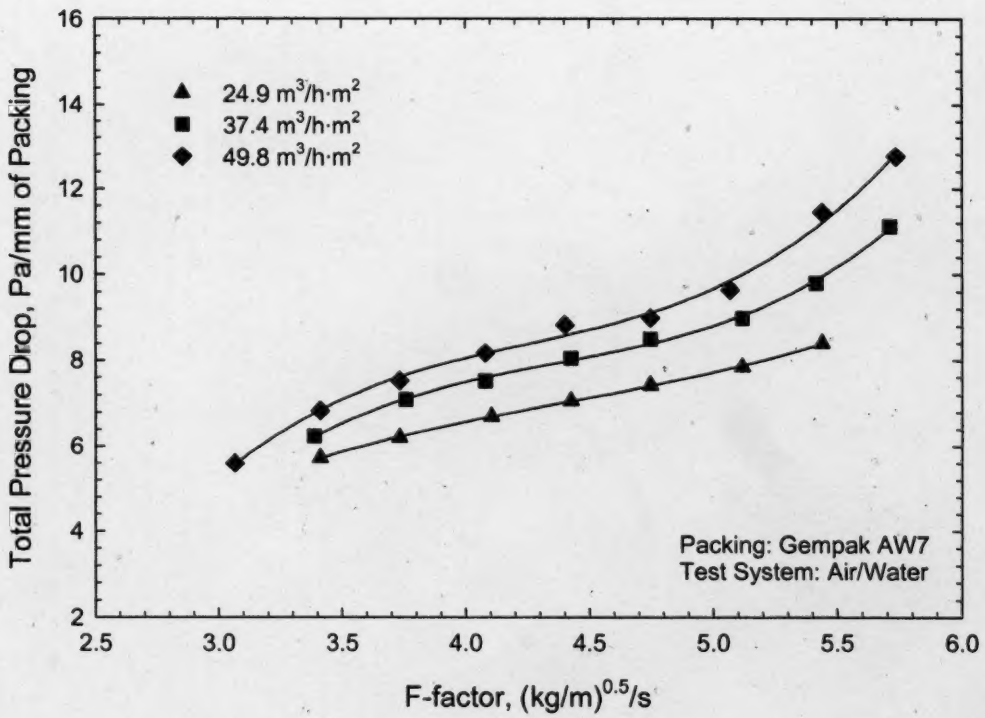

Figure B.4. Comparison of total pressure drop between varying liquid flowrates at a packing thickness of 38.1 mm

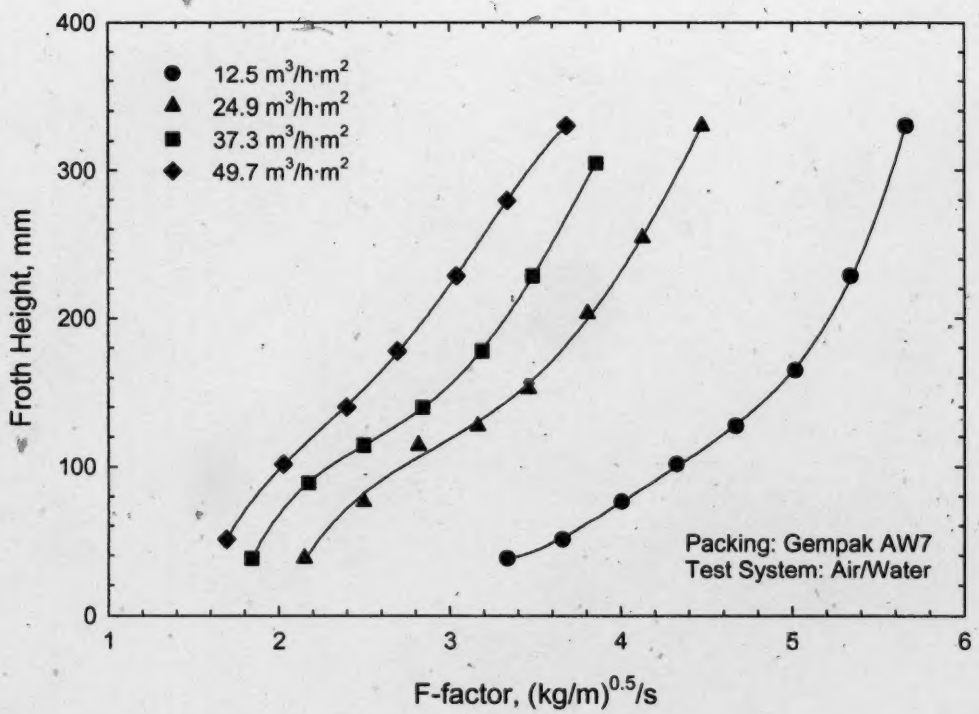

Figure B.5. Comparison of froth height between varying liquid flowrates at a packing thickness of 114.3 mm

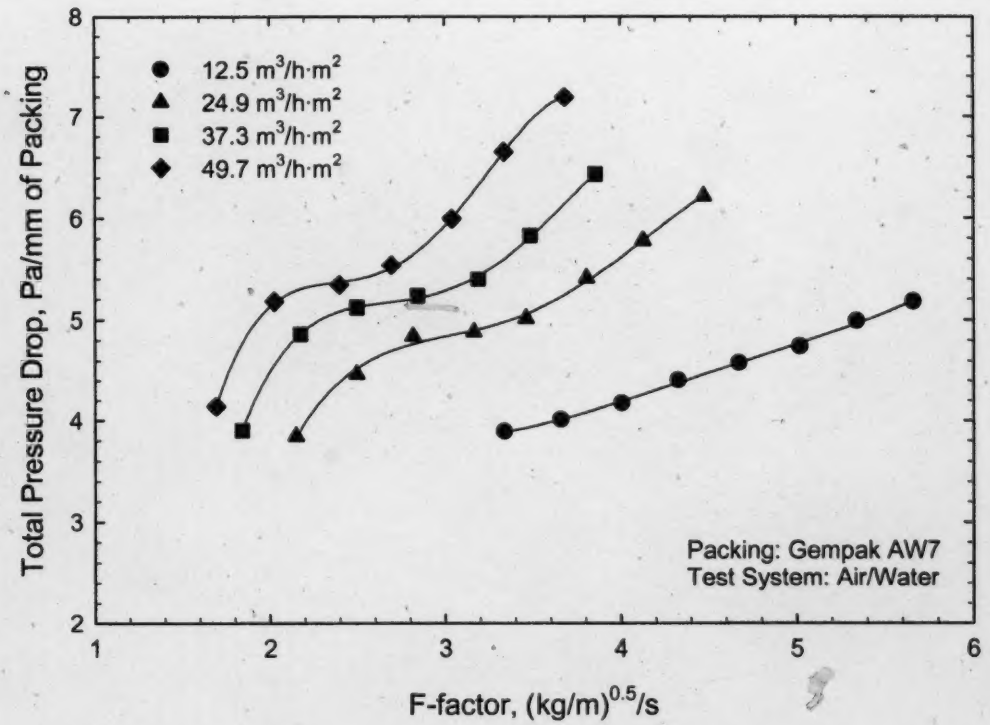

Figure B.6. Comparison of total pressure drop between varying liquid flowrates at a packing thickness of 114.3 mm

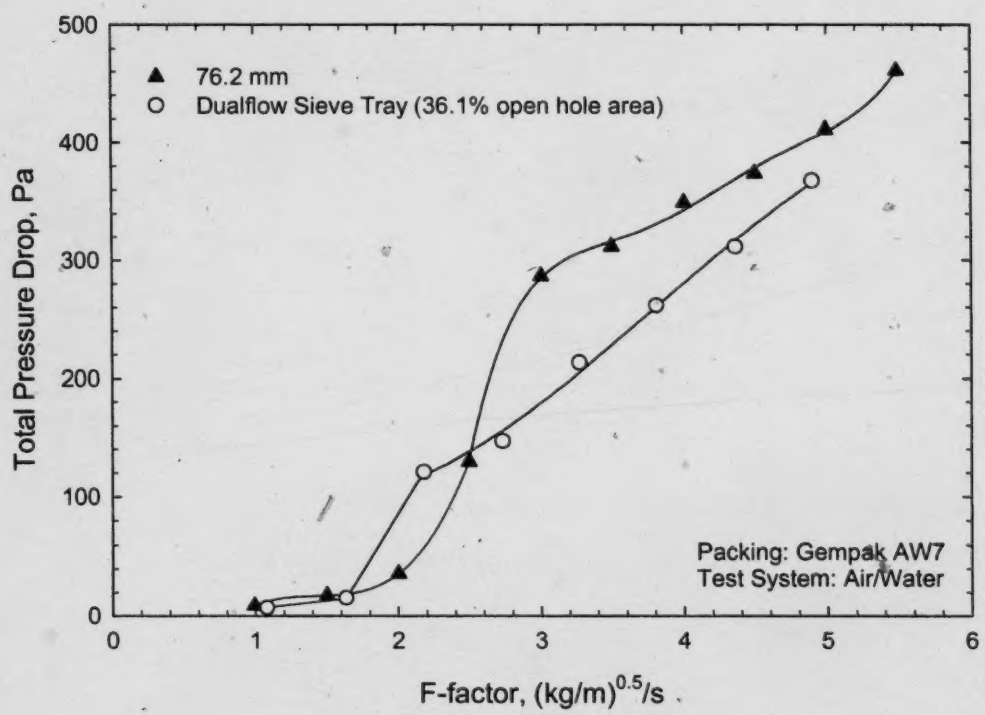

Figure B.7. Comparison of total pressure drop between an SP-tray and a dualflow sieve tray at L/V=1

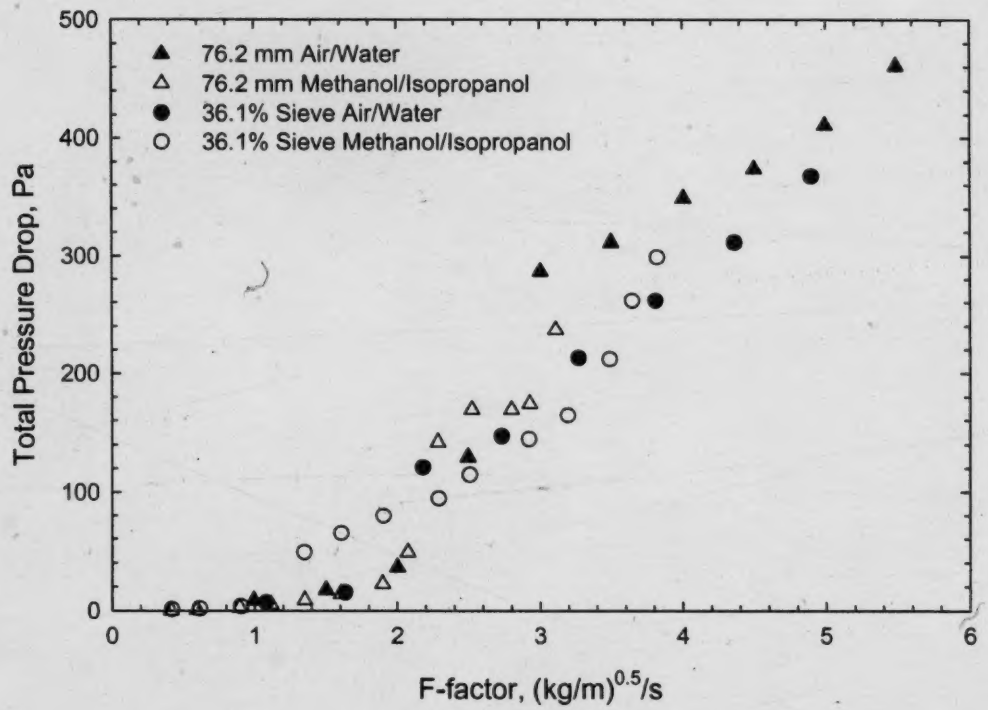

Figure B.8. Comparison of total pressure drop between an SP-tray and a dualflow sieve tray at L/V=1 for different systems

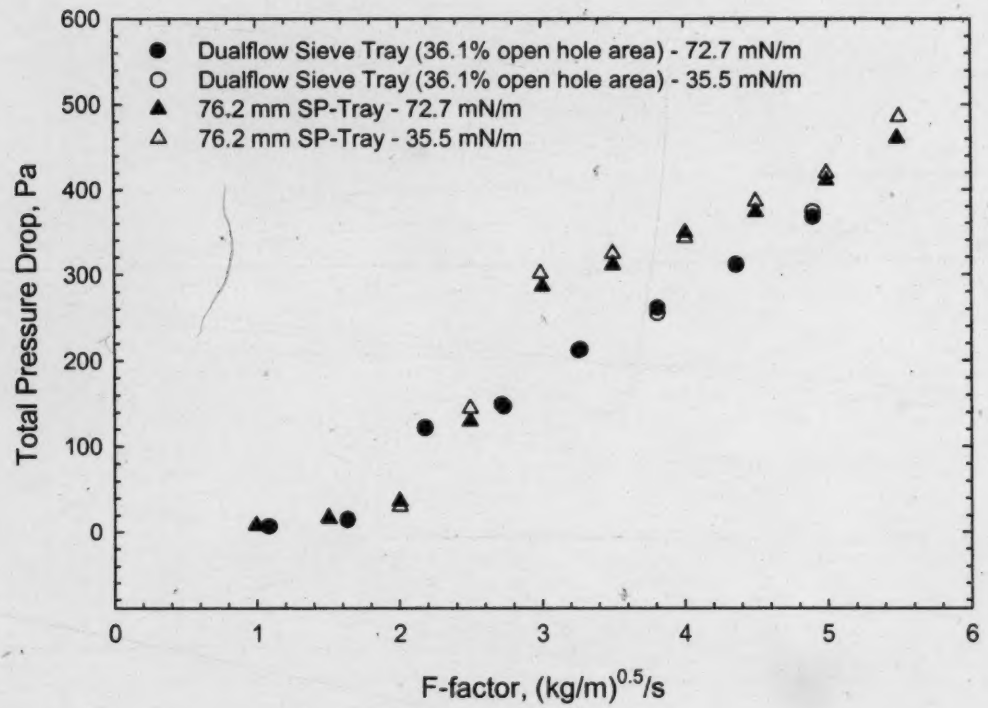

Figure B.9. Effect of surface tension on total pressure drop at L/V=1 in Air/Water System

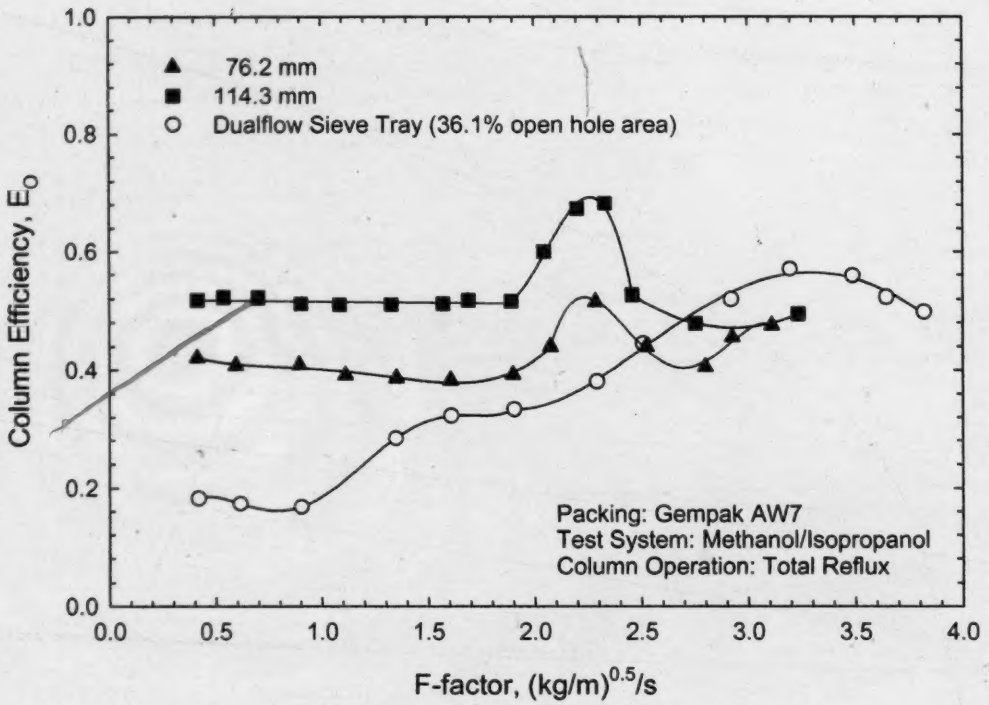

Figure B.10. Comparison of overall column efficiency between varying thickness of packing

Appendix C

SAMPLE CALCULATIONS

Presented below is a set of sample calculations used in determining the calculated values presented. Data used for these calculations is taken from the 76.2 mm SP-tray at the point of peak efficiency.

During operation of the distillation column, the three main sets of data that were recorded were the reflux rate and liquid compositions provided by the gas chromatograph for the liquid into the first tray and exiting the fourth tray. For this analysis, the column provided:

$$\text{Reflux Rate} = 11.4 \text{ kg/min}$$

$$x_{1,in}(\text{area \% MeOH}) = 79.612$$

$$x_{4,out}(\text{area \% MeOH}) = 46.140$$

The gas chromatograph data must first be converted to mass % using the following calibration equation.

$$\text{weight \% MeOH} = 0.00151(\text{area \% MeOH})^2 + 0.85415(\text{area \% MeOH}) - 0.24119$$

As such,

$$x_{1,in}(\text{weight \% MeOH}) = 77.330$$

$$x_{4,out}(\text{weight \% MeOH}) = 42.384$$

In order to determine properties of the methanol/isopropanol system using the data given by Wong (1993), mole fractions must be determined. Using the reflux rate provided and molecular weights of 32.04 and 60.10 kg/kmol for methanol and

isopropanol respectively with the assumption of constant molal overflow (CMO), the mole fractions for each stream are,

$$x_{1,in}(\text{mol \% MeOH}) = 86.484$$

$$x_{4,out}(\text{mol \% MeOH}) = 57.981$$

The F-factor is calculated based on the composition at the top of the column where accurate flow measurements are available from the mass flow meter. An assumption was made stating that the composition of the liquid and vapour streams were identical, i.e. x=y. First, the vapour density is calculated using the following equation.

$$\rho_V = 2.064 - 0.8873(\text{mol fraction MeOH}) = 1.297\ \text{kg/m}^3$$

The column area can be calculated using the column diameter of 0.3048 m.

$$A_C = \frac{\pi D^2}{4} = \frac{\pi(0.3048\ \text{m})^2}{4} = 7.297\text{x}10^{-2}\ \text{m}^2$$

The vapour velocity through the column can now be calculated as

$$U_G = \frac{\dot{m}}{\rho_V A_C} = \frac{(11.4\ \text{kg/min})}{(1.297\ \text{kg/m}^3)(7.297\text{x}10^{-2}\ \text{m}^2)(60\ \text{s/min})} = 2.008\ \text{m/s}$$

Using the vapour velocity and the vapour density the F-factor may now be calculated.

$$\text{F - factor} = U_G\sqrt{\rho_V} = (2.008\ \text{m/s})\sqrt{1.297\ \text{kg/m}^3} = 2.287\ (\text{kg/m})^{0.5}/\text{s}$$

In order to use the Fenske equation, the relative volatility of the methanol/isopropanol mixture must be known. To do so, the relative volatilities at the distillate and bottoms composition must first be calculated. At the bottoms liquid composition of 57.981 mol % MeOH the resulting vapour equilibrium composition of 73.522 mol % MeOH is found. Likewise, at the distillate composition of 86.484 mol% MeOH, a vapour

equilibrium composition of 93.384 mol % MeOH is calculated. This yields relative volatilities of:

$$\alpha_B = \frac{y_B / x_B}{(1-y_B)/(1-x_B)} = \frac{0.73522/0.57981}{(1-0.73522)/(1-0.57981)} = 2.012$$

$$\alpha_D = \frac{y_D / x_D}{(1-y_D)/(1-x_D)} = \frac{0.93384/0.86484}{(1-0.93384)/(1-0.86484)} = 2.206$$

Finding the geometric mean we get,

$$\alpha_{avg} = \sqrt{\alpha_B \alpha_D} = \sqrt{(2.012)(2.206)} = 2.107$$

Since CMO was assumed, both the molar distillate flow rate and bottoms flow rates are identical. The number of theoretical stages can now be calculated using the Fenske equation.

$$N_T = \frac{\ln\left[\left(\frac{x_D}{1-x_D}\right)\left(\frac{1-x_B}{x_B}\right)\right]}{\ln \alpha_{avg}} = \frac{\ln\left[\left(\frac{0.86484}{1-0.86484}\right)\left(\frac{1-0.57981}{0.57981}\right)\right]}{\ln 2.107} = 2.059$$

The overall column efficiency can now be calculated knowing the actual number of stages in the column was four.

$$E_O = \frac{N_T}{N_A} = \frac{2.059}{4} = 0.515$$

The arithmetic mean of the distillate and bottoms compositions is found next.

$$x_{AVG} = \frac{x_D + x_B}{2} = \frac{86.484 + 57.981}{2} = 72.233$$

The slope of the equilibrium line at this point is found using the derivative of the equilibrium correlation and gives a slope of 0.690. The Murphree tray efficiency can now be calculated keeping in mind that V/L=1 for total reflux operation.

$$E_{MV} = \frac{\lambda^{E_o} - 1}{\lambda - 1} = \frac{0.690^{0.515} - 1}{0.690 - 1} = 0.561$$

The value of the HETP can be calculated by assuming that four 76.2 mm SP-trays are equivalent to 304.8 mm of total packing.

$$HETP = \frac{z}{N_T} = \frac{(0.3048\,m)}{2.059} = 0.148\,m$$